

Parameterizing empirical interatomic potentials for predicting thermophysical properties via an irreducible derivative approach: the case of ThO₂ and UO₂

Shuxiang Zhou^{1,*}, Chao Jiang¹, Enda Xiao², Sasaank Bandi³, Michael W.D. Cooper⁴,
Miaomiao Jin⁵, David H Hurley¹, Marat Khafizov⁶, and Chris A. Marianetti³

¹*Idaho National Laboratory, Idaho Falls, ID 83415, USA*

²*Department of Chemistry, Columbia University, New York, NY 10027, USA*

³*Department of Applied Physics and Applied Mathematics,
Columbia University, New York, NY 10027, USA*

⁴*Los Alamos National Laboratory, Los Alamos, NM 87545, USA*

⁵*Department of Nuclear Engineering, The Pennsylvania State University, University Park, PA 16802, USA*

⁶*Department of Mechanical and Aerospace Engineering,
The Ohio State University, Columbus, OH 43210, USA*

The accuracy of classical physical property predictions using molecular dynamics simulations is determined by the quality of the interatomic potentials. Here we introduce a training approach for empirical interatomic potentials (EIPs) which is well suited for capturing phonons and phonon-related properties. Our approach is based on direct comparisons of the second- and third-order irreducible derivatives between an EIP and the Born-Oppenheimer potential within density functional theory (DFT) calculations. Irreducible derivatives fully exploit space group symmetry and allow for training without redundant information. We demonstrate the fidelity of our approach in the context of ThO₂ and UO₂, where we optimize parameters of an embedded-atom method potential in addition to core-shell interactions. Our EIPs provide thermophysical properties in good agreement with DFT and outperform widely utilized EIPs for phonon dispersion and thermal conductivity predictions. Reasonable estimates of thermal expansion and formation energies of Frenkel pairs are also obtained.

I. INTRODUCTION

Interatomic potentials are mathematical models used to encode the Born-Oppenheimer potential of some collection of atoms. Traditionally, empirical interatomic potentials (EIPs) are derived using analytical functional forms with a few parameters: examples include the Lennard-Jones potential [1], which has only two parameters in simple systems, and the Tersoff potential [2] and embedded atom method (EAM) potential [3], which both have tens of parameters. The analytical functional forms and the limited number of parameters of EIPs offer simplicity for modeling, but also restrict accuracy and limit the potential for capturing complex phenomena. Recently, machine-learning interatomic potentials (MLIPs) have emerged as a valuable complement to traditional EIPs by leveraging machine-learning algorithms like neural networks and Gaussian process regression [4, 5], exhibiting higher accuracy and transferability. However, MLIPs are computationally more demanding, often using thousands to millions of parameters. Despite the success of MLIPs, EIPs are still useful given their computational efficiency and physical interpretability.

In the last few decades, extensive studies have been performed to advance the training procedure for interatomic potentials. EIPs were previously trained by fitting to experimental measurements, including the lattice parameters, elastic constants, thermal expansion, and

specific heat [2, 3, 6, 7]. As training data, experimental measurements are limited by both quantity and quality. In terms of quantity, experiments are often limited by high-cost and time-consuming processes, especially for complex systems such as defect structures. Additionally, experiments are limited in terms of directly probing the details of the Born-Oppenheimer potential, and instead only measure averaged quantities. This lack of data can limit the accuracy of the EIP and can yield substantial errors for selected observables. For example, traditional parametrization of EIPs to elastic constants and thermal expansion is often inadequate for accurately predicting phonon dispersions, not to mention third-order phonon interactions [8]. Both the challenge of quantity and quality of training data can be resolved by utilizing first-principles calculations, where approaches such as density functional theory (DFT) can produce a multitude of atomistic data at both equilibrium and non-equilibrium.

Given that the goal of parameterizing an interatomic potential is to faithfully encode the Born-Oppenheimer potential, a natural source of training data would be a direct sampling of the Born-Oppenheimer potential over some relevant domain, which can be achieved when using data from sufficiently reliable first-principles calculations. There are various approaches for sampling the Born-Oppenheimer potential. One approach would be to compute the value of the Born-Oppenheimer potential (i.e. energy) and the first derivatives (i.e. forces) at a collection of configurations, which is practical for approaches such as density functional theory where the forces can be computed at a small computational overhead. The collection of configurations might be gener-

* shuxiang.zhou@inl.gov

ated using a molecular dynamics trajectory. EIPs trained on DFT-calculated energies and forces have generated robust results, including reasonable predictions of phonons [9–19] and defect energies [20], and it is standard to train MLIP on DFT-calculated forces and energies [21]. An alternative approach would be to use a single minimum energy configuration and construct the second and third derivatives of the Born-Oppenheimer potential of this configuration. The use of second- and higher-order derivatives in potential training is relatively uncommon compared to the utilization of energies and forces, both due to the increased computational cost of generating the data and training the model. However, if the targeted observables to be generated using the EIP directly probe the derivatives (e.g. scattering function), using the second and higher order derivatives as training data may be worthwhile. For example, interatomic potentials trained using DFT-calculated second energy derivatives can significantly improve the predicted phonon dispersion, for both EIP [22–28] and MLIP [29, 30]. When training to second- and higher-order energy derivatives, it is important not to have any redundancy in the training data, which can be achieved using space group irreducible derivatives (ID) [31]. The IDs are generated using the group theoretical selection rules which dictate which irreducible representations are allowed to couple, providing a minimal set of derivatives that characterize a given discretization of the Brillouin zone.

In this work, we develop an ID-based potential training approach, by including the second- and third-order displacement IDs and the second-order strain IDs in the training data. Our approach is used to parameterize an EIP for the nuclear fuel materials ThO₂ and UO₂, where there is a critical need to understand defect formation, microstructure evolution, and thermal transport degradation [32–44]. A previously developed EIP for the actinide oxides [7], referred to as the CRG potential, has found widespread use in classical molecular dynamics (MD) studies of actinide oxides [45–55]. The CRG potential was parameterized in a traditional fashion, based on the experimental elastic constant and thermal expansion. Recently, the accuracy of the CRG potential for predicting phonons and thermal transport within the Boltzmann transport equation (BTE) framework was assessed, demonstrating that the CRG potential has nontrivial differences with the experimental phonon dispersion of optical branches as well as with the thermal conductivity [56]. These differences are not unexpected, given that neither the phonons nor the phonon interactions were included in the CRG training data. In this work, we demonstrate that our ID-based training procedure yields an EIP that reliably characterizes the first-principles data. Given that DFT and DFT+*U* can reliably describe ThO₂ and UO₂ [34, 57–60], respectively, our resulting EIP yields a substantial improvement over the CRG potential for the predicted phonon related properties relative to experiment.

II. METHODS

A. Potential form

In this work, the analytical expression of the EIP is based on the CRG potential [7], which uses a pair-potential for each atom pair in addition to the many-body EAM potential [3]. The pair-potential contains three contributions: the Buckingham potential [61], the Morse potential [62], and the long-range electrostatic Coulomb interaction. Additionally, a core-shell spring model [63] is added, as it substantially improves the prediction of selected optical phonons. Within the core-shell model, each ion splits into two particles, a core and a shell, where the core and shell are attached by a spring force with spring constant k (see the last term of Eq. 1). The charge and mass of the ion also split into a core and shell contribution, and here we apply the massless shell model, as implemented in the General Utility Lattice Program (GULP) package [64]. The non-Coulombic interactions (i.e., Buckingham potential, Morse potential, and EAM) are only defined between the shells, while Coulombic interactions are applied between all cores and shells, except the core and shell of the same ion (see Eq. 3).

We denote the distances between the core-shell ion i and j as a vector $\mathbf{r}_{ij} = (r_{ij}^{cc}, r_{ij}^{cs}, r_{ij}^{sc}, r_{ij}^{ss})$, where r_{ij}^{cc} , r_{ij}^{cs} , r_{ij}^{sc} , r_{ij}^{ss} represent the distance between i 's core and j 's core, i 's core and j 's shell, i 's shell and j 's core, and i 's shell and j 's shell, respectively. The potential energy E_i of an ion i concerning all other ions is given by:

$$E_i = \frac{1}{2} \sum_{j \neq i} \phi_{\alpha\beta}(\mathbf{r}_{ij}) - G_\alpha \sqrt{\sum_{j \neq i} \sigma_\beta(r_{ij}^{ss})} + \frac{1}{2} k_i r_{ii}^{cs2}, \quad (1)$$

which is a sum of pairwise components, many-body components, and harmonic spring component terms. The pairwise potential between ions i and j , $\phi_{\alpha\beta}(\mathbf{r}_{ij})$, is given by the sum of the Coulomb potential $\phi_C(\mathbf{r}_{ij})$, the Buckingham potential $\phi_B(r_{ij}^{ss})$, and the Morse potential $\phi_M(r_{ij}^{ss})$:

$$\phi_{\alpha\beta}(\mathbf{r}_{ij}) = \phi_C(\mathbf{r}_{ij}) + \phi_B(r_{ij}^{ss}) + \phi_M(r_{ij}^{ss}), \quad (2)$$

$$\phi_C(\mathbf{r}_{ij}) = \frac{1}{4\pi\epsilon_0} \left(\frac{q_\alpha^c q_\beta^c}{r_{ij}^{cc}} + \frac{q_\alpha^c q_\beta^s}{r_{ij}^{cs}} + \frac{q_\alpha^s q_\beta^c}{r_{ij}^{sc}} + \frac{q_\alpha^s q_\beta^s}{r_{ij}^{ss}} \right), \quad (3)$$

$$\phi_B(r_{ij}^{ss}) = A_{\alpha\beta} \exp\left(\frac{-r_{ij}^{ss}}{\rho_{\alpha\beta}}\right) - \frac{C_{\alpha\beta}}{(r_{ij}^{ss})^6}, \quad (4)$$

$$\phi_M(r_{ij}^{ss}) = D_{\alpha\beta} [e^{-2\gamma_{\alpha\beta}(r_{ij}^{ss}-r_0)} - 2e^{-\gamma_{\alpha\beta}(r_{ij}^{ss}-r_0)}], \quad (5)$$

where α and β are the labels of species for ions i and j , respectively. The many-body term in Eq. (1) is given by the square root of the sum of the pairwise function $\sigma_\beta(r_{ij}^{ss})$, given by:

$$\sigma_\beta(r_{ij}^{ss}) = \frac{n_\beta}{r_{ij}^{ss8}}. \quad (6)$$

TABLE I. Parameters for the short-range pairwise potentials described by Eqs. (4)–(5).

Interaction	$\phi_B(r_{ij})$			$\phi_M(r_{ij})$		
	$A_{\alpha\beta}(\text{eV})$	$\rho_{\alpha\beta}(\text{\AA})$	$C_{\alpha\beta}(\text{eV}\text{\AA}^6)$	$D_{\alpha\beta}(\text{eV})$	$\gamma_{\alpha\beta}(\text{\AA}^{-1})$	$r_0(\text{\AA})$
Th-Th	16 078.23	0.2985	1.6499	5.0866	5.7739	2.4611
U-U	18 447.13	0.1452	12.9937	6.2571	4.2394	2.1289
Th-O	859.98	0.3820	9.7412	0.3241	2.1530	2.4440
U-O	807.24	0.3895	6.0011	0.3088	1.9770	2.5195
O-O	958.50	0.3202	7.0602	-	-	-

TABLE II. Parameters for the many-body term, the Coulomb potential, and core-shell models described by Eqs. (1), (3), and (6).

Species	$G_\alpha(\text{eV}\text{\AA}^{1.5})$	$n_\alpha(\text{\AA}^5)$	$q_\alpha^c(e)$	$q_\alpha^s(e)$	$k_\alpha(\text{eV}\text{\AA}^{-2})$
Th	1.1122	899.84	-9.7268	12.6813	1204.99
U	2.0053	991.90	-7.2900	10.2445	551.98
O	0.4772	986.88	1.7688	-3.2461	436.86

B. Training procedure and model assessment

Due to the specific interests in phonon predictions, our dataset was separated into two categories, phonon-related properties and other properties. Phonon-related properties contain the second-order displacement IDs, the third-order displacement IDs, the second-order strain IDs, and phonon thermal conductivity. Besides these phonon-related properties, we consider the classical lattice parameter $a(T)$ at $T = 0$ K, the normalized Born effective charges Z_α^* , and the defect formation energy (E_F) of Frenkel pairs (FPs). Here Z_α^* is obtained by the Born effective charge Z_α normalized by the dielectric constant ϵ : $Z_\alpha^* = Z_\alpha/\sqrt{\epsilon}$. Among the different types of point defects, only the FP is considered, so a direct comparison can be made between DFT and the EIP, avoiding approximations needed to treat unbalanced charges. The training dataset contained the second-order displacement IDs within the $2 \times 2 \times 2$ supercell, the third-order displacement IDs within the conventional cubic supercell $\hat{\mathbf{S}}_C$, the second-order strain IDs, $a(0)$, Z_α^* , and E_F for a Th or U FP in the conventional cubic supercell, while the remaining data were used to assess the accuracy of the model. The details of properties used in the training procedure and assessment are tabulated in Table S1 of the Supplemental Materials (SM) [65]. Additionally, we also predicted thermal expansion using the EIP and directly compared with experimental results. See Section I of SM [65] for the mathematical representation of the supercells used in calculations, following Ref.[31].

All DFT calculations were carried out via a projector augmented-wave (PAW) method [66, 67], as implemented in the Vienna ab initio simulation package [68, 69]. For the exchange-correlation functionals, the strongly con-

strained and appropriately normed (SCAN) [70] functional was used for ThO_2 , while the Perdew, Burke, Ernzerhof (PBE) generalized gradient approximation (GGA) [71] was used for UO_2 , following previous DFT studies [34, 57–60, 72] which yield phonons in good agreement with experiments. Additionally, the UO_2 calculations applied spin-orbit coupling, DFT+ U [73, 74] with $U = 4$ eV, and occupation matrix control with the initial values of the occupation matrices from the $3\mathbf{k}$ AFM state reported in Ref. [59]. The plane-wave cutoff energy was set to 550 eV, and the energy convergence criterion was set to 10^{-6} eV. For the primitive cell, a Γ -centered $13 \times 13 \times 13$ k -point mesh [75] was applied; for supercells, the k -point densities were kept approximately the same. The second-order displacement IDs and the second-order strain IDs were calculated using the lone irreducible derivative approach, and the third-order displacement IDs were calculated using the bundled irreducible derivative approach [31]. All second-order displacement IDs (phonon dispersion) commensurate with the $4 \times 4 \times 4$ supercell were computed, while all third-order displacement IDs commensurate with the non-diagonal supercell $\hat{\mathbf{S}}_O$ were computed. The thermal conductivity is computed within the relaxation time approximation (RTA) using a $12 \times 12 \times 12$ \mathbf{q} -mesh. The formation energy E_F of FPs is computed with the volume fixed, while the interstitial is located in the octahedral site.

The GULP package [64] was applied to calculate the static properties of EIPs, including lattice parameter, force, energy, dielectric constant, and Born effective charge. The Coulomb interactions were implemented using the Ewald summation [76], where an 11.0 \AA cut-off was applied for both the pairwise and many-body interactions. For thermal expansion, MD simulations were performed by GULP in an NPT ensemble at T up to 3000 K using the non-diagonal supercell $4\hat{\mathbf{S}}_C$. Each MD simulation runs 5 ps with a time step of 2 fs, while $a(T)$ is obtained by averaging the last 4 ps.

The parameter optimization for the EIPs was carried out using the Potential Pro-Fit package [77], which minimizes the total error e , given by:

$$e = \sqrt{\sum (w_i e_i)^2}, \quad (7)$$

where w_i and e_i are the weight and error, respectively, for the i -th training data. The parameter optimization

TABLE III. A portion of training data, including the second-order displacement IDs, the second-order strain IDs, lattice parameter at $T = 0$ (denoted $a(0)$), normalized Born effective charges Z_{Th}^* or Z_U^* , and the defect formation energy E_F for a Th or U FP in the conventional cubic supercell, computed by DFT, and compared with the CRG [7] and the PW.

Property	ThO ₂			UO ₂		
	SCAN	CRG	PW	PBE+ U	CRG	PW
Second-order irreducible derivatives within the $2 \times 2 \times 2$ supercell (eV/Å ²)						
$d_{\Gamma\Gamma}^{T_{2g}T_{2g}}$	12.65	16.02	12.82	11.64	17.35	12.90
$d_{\Gamma\Gamma}^{T_{1u}T_{1u}}$	12.75	16.60	11.62	10.91	15.63	10.06
$d_{LL}^{A_{1g}A_{1g}}$	17.47	16.28	16.87	16.11	17.34	17.67
$d_{LL}^{E_gE_g}$	9.57	11.10	9.14	8.69	11.64	9.01
$d_{LL}^{A_{2u}A_{2u}}$	35.76	32.75	34.01	30.50	32.04	28.83
$d_{LL}^{A_{2u}^1A_{2u}^1}$	7.78	6.69	5.73	6.63	7.72	4.14
$d_{LL}^{A_{2u}^1A_{2u}^1}$	10.07	16.10	9.97	8.72	17.14	8.36
$d_{LL}^{E_uE_u}$	9.59	12.22	9.62	7.93	11.25	8.15
$d_{LL}^{E_u^1E_u^1}$	-3.09	-6.57	-3.19	-2.62	-5.85	-2.49
$d_{LL}^{E_u^1E_u^1}$	7.55	11.10	7.47	6.89	11.64	6.75
$d_{XX}^{A_{1g}A_{1g}}$	21.02	27.18	25.23	19.74	29.87	26.53
$d_{XX}^{E_gE_g}$	4.61	4.11	3.03	3.70	3.55	2.57
$d_{XX}^{2A_{2u}2A_{2u}}$	41.53	28.64	31.60	37.25	28.23	26.95
$d_{XX}^{B_{1u}B_{1u}}$	2.53	2.86	1.91	1.55	2.10	1.39
$d_{XX}^{E_uE_u}$	12.09	19.62	12.79	11.38	21.45	11.68
$d_{XX}^{E_u^1E_u^1}$	-0.59	-4.12	-0.63	-0.24	-3.13	-0.23
$d_{XX}^{E_u^1E_u^1}$	11.79	14.76	13.67	9.40	13.33	11.69
Elastic energy irreducible strain derivatives (eV)						
$d_{A_{1g}A_{1g}}$	166.73	157.02	166.52	164.91	165.92	165.88
$d_{E_gE_g}$	70.81	64.78	68.89	69.48	71.25	66.55
$d_{T_{2g}T_{2g}}$	22.13	19.43	20.56	16.66	16.17	16.33
Other properties						
$a(0)$ (Å)	5.594	5.580	5.594	5.546	5.453	5.546
Z_{Th}^* or Z_U^* ($ e $)	2.448	2.221	2.448	2.325	2.221	2.325
E_F (Th or U FP) (eV)	18.000	17.529	17.999	14.023	11.165	14.033

method was provided as a flowchart in Section II of SM [65], and the weight of training data is tabulated in Table S1 of SM [65]. Throughout this work, we denote our trained EIP as the present work (PW), and its optimized parameter values are presented in Tables I and II. To demonstrate the robustness of our training method, two alternative potential forms without the core-shell model have also been trained, and improvements of thermophysical predictions relative to the CRG potential are also observed (see in Section VII of SM [65]).

III. RESULTS AND DISCUSSIONS

We begin by comparing the PW with the DFT training and assessment data to ensure that a good fit was achieved. For training data, the comparison is tabulated in Table III, except the third-order displacement IDs which are tabulated in Table S2 of SM [65]. For the assessment data, the comparison for each property can be found by using Table S1 of SM [65], including the second- and third-order displacement IDs in larger supercells, the formation energy for FPs in larger supercells, and thermal conductivity computed by using the BTE within the RTA. Overall, our parameter optimization process yields an EIP with relatively small errors relative to the DFT data. Interestingly, while the PW only has two training

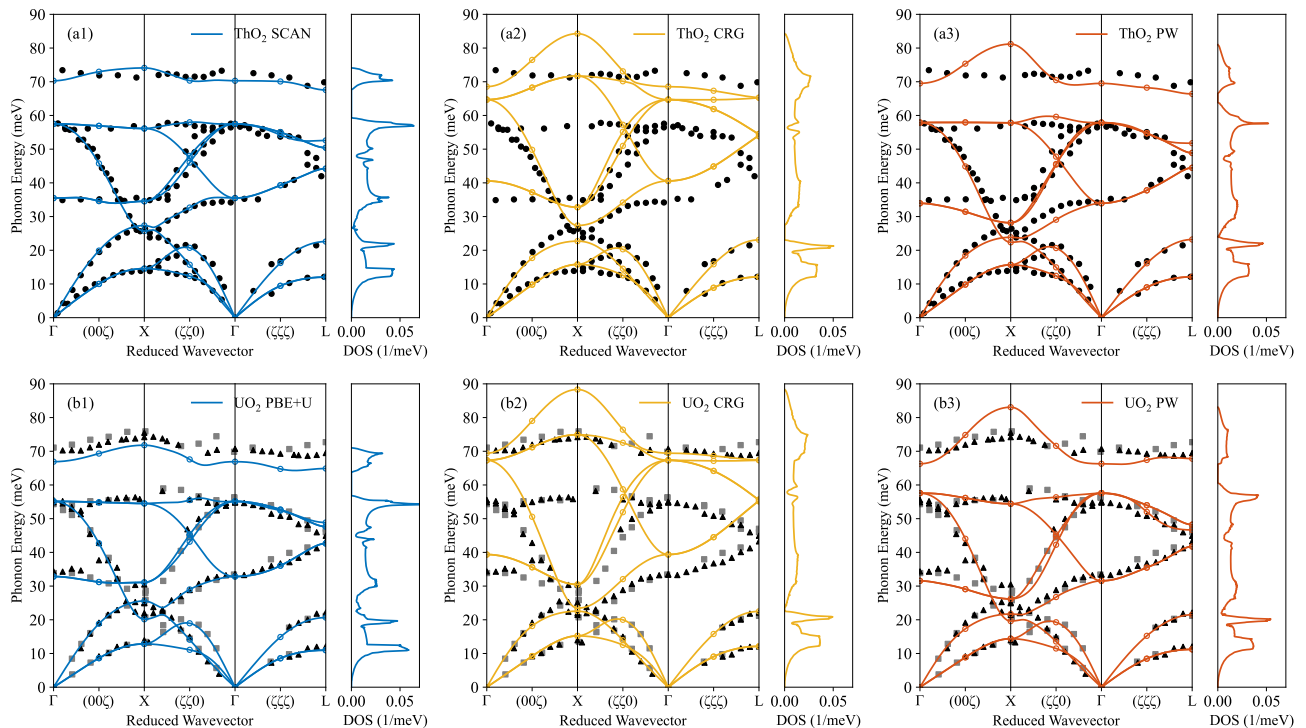


FIG. 1. Calculated phonon dispersion and density of states for (a) ThO_2 and (b) UO_2 , by using (1) DFT, (2) the CRG, and (3) the PW, compared to experimental data of ThO_2 (black circles) [78] and UO_2 (grey squares [79] and black triangles [60]). The lines are a Fourier interpolation of the computed data points, which are presented as open circles.

data points for the defect formation energy (i.e., FP of Th or U in a conventional cell of ThO_2 or UO_2 , respectively), the PW can predict the formation energies for FPs of O, Th, and U in a larger supercell ($2 \times 2 \times 2$ of the conventional cell) reasonably well, all within 9% error compared with DFT (see Table IV). For the sake of comparison, all of the aforementioned properties are also computed using the CRG.

We proceed to assess the PW via comparison with experiments and the CRG potential, which is fitted to experimental elastic constants and thermal expansion. For the phonon dispersion, Figure 1 presents the comparison between DFT, EIPs, and experiments [59, 78, 79]. The CRG potential exhibits two deficiencies: the overprediction of all optical phonon branches and the inability to capture the phonon frequency gap between the highest two optical branches. As DFT can accurately capture the phonon dispersion in comparison with experiments, the PW, which is fitted to DFT, significantly improves the agreement of the optical phonon branches. Furthermore, a gap between the highest two optical branches is successfully predicted, which can be attributed to the core-shell model (see Section VII of SM [65] for more details). The only major deficiency of the PW for the phonon dispersion is the overprediction of the highest optical branch near the X point. However, as the highest phonon branch has a negligible contribution to the thermal conductivity in ThO_2 and UO_2 [56, 58, 60], this error should not signif-

icantly affect the thermal transport (see Section VI of SM [65] for more details). Table IV tabulates the calculated elastic constants. Compared with experiments [80–82], the PW has better predictions than the CRG for C_{11} and C_{44} in ThO_2 , and C_{44} in UO_2 , though the CRG was directly fitted to experimental elastic constants. For the predictions of C_{12} in ThO_2 and C_{11} in UO_2 , the PW is not as good as the CRG, but this is mainly due to the discrepancy between DFT and experiments. The thermal conductivity is computed and compared with experiments [38, 83–88] in Figure 2. The PW significantly improves the thermal conductivity prediction as compared to the CRG, which is expected given that DFT has good agreement with experiments. For example, at $T = 1000$ K, the errors of predicted thermal conductivity by the CRG for ThO_2 and UO_2 are 54% and 63%, respectively, which are reduced to 17% and 9% by the PW, respectively, compared with experiments (see Section VI of SM [65] for more details). Finally, we compare the thermal expansion predictions with experiments [85, 89]. As the CRG and the PW predict different $a(0)$, rather than comparing a directly, we compare the percentage change in lattice parameter, $\frac{a(T)-a(0)}{a(0)}$ (see in Figure 3), with experiments. The PW gives good agreement with experiment up to $T = 2500$ K for both ThO_2 and UO_2 , and slightly underpredicts the lattice parameter when $T > 2500$ K. In summary, the PW yields good agreement with the DFT data of irreducible derivatives, $a(0)$, Z_α^* , the forma-

TABLE IV. Elastic constants and defect formation energy E_F for FPs calculated using DFT, the CRG, and the PW in comparison to experimental data [80–82]. See Section IV of SM for definitions of FP1 and FP2 [65].

Property	ThO ₂				UO ₂			
	SCAN	CRG	PW	exp	PBE+U	CRG	PW	exp
Elastic constants (GPa)								
C_{11}	376	352	371	367 ^a , 366 ^b	380	406	374	400 ^c
C_{12}	117	113	119	106 ^a , 114 ^b	120	125	124	125 ^c
C_{44}	81	72	75	80 ^a , 81 ^b	63	64	61	59 ^c
Defect formation energy E_F (eV)								
O FP1	4.55	5.25	4.78		4.02	5.36	4.30	
O FP2	4.63	5.61	4.95		4.06	5.77	4.41	
Th or U FP	13.15	13.63	13.93		10.26	11.07	10.62	

^a Ref. [80], ^b Ref. [81], ^c Ref. [82].

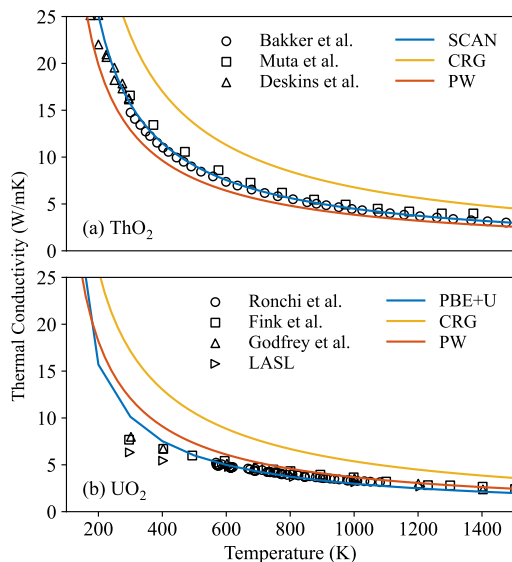


FIG. 2. Calculated phonon thermal conductivity obtained from the BTE within the RTA for (a) ThO₂ and (b) UO₂, using DFT, the CRG, and the PW at $T = 100 - 1500$ K, compared with the experimental data of ThO₂ [38, 83, 84] and UO₂ [85–88].

tion energy of FPs, and thermal conductivity. Compared with experiments, the PW also outperforms the CRG for phonon dispersions, elastic constants, and thermal conductivity, except for certain elastic constants where DFT has discrepancies with experiments, and thermal expansion at high temperatures where there is likely insufficient training data.

IV. CONCLUSION

In this work, we developed an interatomic potential training approach by utilizing irreducible derivatives

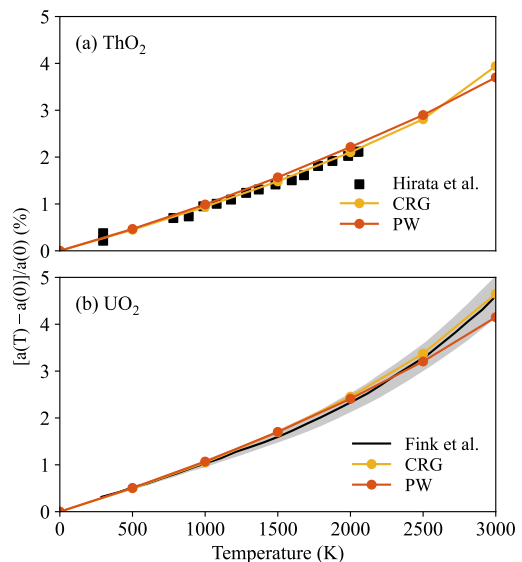


FIG. 3. Calculated percentage change of the lattice parameter as a function of temperature at $T = 0 - 3000$ K obtained from molecular dynamics simulations for (a) ThO₂ and (b) UO₂ using the CRG and the PW, compared with the experimental data of ThO₂ [89] and UO₂ [85].

(IDs), including second- and third-order displacement IDs and second-order strain IDs, calculated from DFT. This ID-based potential training approach was used to construct an empirical interatomic potential (EIP) for ThO₂ and UO₂ crystals, yielding an EIP with relatively small errors relative to the DFT data, including the aforementioned IDs, phonon dispersion, thermal conductivity, and the formation energy of Frenkel pairs. Compared with experiments, the PW outperforms the widely-used CRG potential [7] for phonon dispersions and thermal conductivity. In addition to using a far more expansive training data set for our EIP, we also enhanced the analytical functional form for our EIP to include a core-shell

model, which was essential for capturing selected optical phonon modes. Training EIPs based on IDs is clearly a promising direction for developing accurate interatomic potentials focussed on predicting phonon-related thermophysical properties, and this approach will likely be useful in the broader context of machine learning-based potentials.

V. ACKNOWLEDGEMENTS

This work was supported by the Center for Thermal Energy Transport under Irradiation, an Energy Frontier Research Center funded by the U.S. Department of Energy (DOE) Office of Basic Energy Sciences. This re-

search made use of the resources of the High Performance Computing Center at Idaho National Laboratory, which is supported by the Office of Nuclear Energy of the U.S. Department of Energy and the Nuclear Science User Facilities under Contract No. DE-AC07-05ID14517. M.W.D.C. acknowledges support from the Nuclear Energy Advanced Modeling and Simulation (NEAMS) Program funded by the U.S. DOE Office of Nuclear Energy. S.B., E.X., and C.A.M. acknowledge resources of the National Energy Research Scientific Computing Center, a DOE Office of Science User Facility supported by the Office of Science of the U.S. Department of Energy under Contract No. DE-AC02-05CH11231. Grant DE-SC0016507 supported S.B. and C.A.M. for integrating empirical potentials in the irreducible derivative framework.

-
- [1] J. E. Lennard-Jones, Proceedings of the Physical Society **43**, 461 (1931).
- [2] J. Tersoff, Physical Review B **38**, 9902 (1988).
- [3] M. S. Daw and M. I. Baskes, Physical Review B **29**, 6443 (1984).
- [4] J. Behler and M. Parrinello, Physical Review Letters **98**, 146401 (2007).
- [5] A. P. Bartók, M. C. Payne, R. Kondor, and G. Csányi, Physical Review Letters **104**, 136403 (2010).
- [6] M. P. Allen and D. J. Tildesley, *Computer Simulation of Liquids: Second Edition* (Oxford, 2017).
- [7] M. W. D. Cooper, M. J. D. Rushton, and R. W. Grimes, Journal of Physics: Condensed Matter **26**, 105401 (2014).
- [8] A. Chernatynskiy, C. Flint, S. Sinnott, and S. Phillpot, Journal of Materials Science **47**, 7693 (2012).
- [9] F. Ercolessi and J. B. Adams, Europhysics Letters **26**, 583 (1994).
- [10] Y. Mishin, D. Farkas, M. Mehl, and D. Papaconstantopoulos, Physical Review B **59**, 3393 (1999).
- [11] M. R. Fellingner, H. Park, and J. W. Wilkins, Physical Review B—Condensed Matter and Materials Physics **81**, 144119 (2010).
- [12] Y. Lee and G. S. Hwang, Physical Review B—Condensed Matter and Materials Physics **85**, 125204 (2012).
- [13] P. Brommer, A. Kiselev, D. Schopf, P. Beck, J. Roth, and H.-R. Trebin, Modelling and Simulation in Materials Science and Engineering **23**, 074002 (2015).
- [14] D. Schopf, H. Euchner, and H.-R. Trebin, Physical Review B **89**, 214306 (2014).
- [15] Z. Fan, Y. Wang, X. Gu, P. Qian, Y. Su, and T. Ala-Nissila, Journal of Physics: Condensed Matter **32**, 135901 (2019).
- [16] B. Qiu and X. Ruan, Physical Review B **80**, 165203 (2009).
- [17] P. Roy Chowdhury, T. Feng, and X. Ruan, Physical Review B **99**, 155202 (2019).
- [18] Z. Fan, Y. Wang, X. Gu, P. Qian, Y. Su, and T. Ala-Nissila, Journal of Physics: Condensed Matter **32**, 135901 (2019).
- [19] K. Tanaka, Y. Sakai, S. Taniguchi, K. Shimomai, and Y. Iwazaki, Journal of the Ceramic Society of Japan **131**, 252 (2023).
- [20] M. W. D. Cooper, N. Kuganathan, P. A. Burr, M. J. D. Rushton, R. W. Grimes, C. R. Stanek, and D. A. Andersson, Journal of Physics: Condensed Matter **28**, 405401 (2016).
- [21] I. S. Novikov, K. Gubaev, E. V. Podryabinkin, and A. V. Shapeev, Machine Learning: Science and Technology **2**, 025002 (2020).
- [22] L. Lindsay and D. Broido, Physical Review B—Condensed Matter and Materials Physics **81**, 205441 (2010).
- [23] T. Murakami, T. Shiga, T. Hori, K. Esfarjani, and J. Shiomi, EPL (Europhysics Letters) **102**, 46002 (2013).
- [24] P. Han and G. Bester, Physical Review B **83**, 174304 (2011).
- [25] A. Rohskopf, H. R. Seyf, K. Gordiz, T. Tadano, and A. Henry, npj Computational Materials **3**, 1 (2017).
- [26] M. G. Muraleedharan, A. Rohskopf, V. Yang, and A. Henry, AIP Advances **7** (2017).
- [27] A. Rohskopf, S. Wyant, K. Gordiz, H. R. Seyf, M. G. Muraleedharan, and A. Henry, Computational Materials Science **184**, 109884 (2020).
- [28] L. Shi, X. Ma, M. Li, Y. Zhong, L. Yang, W. Yin, and X. He, Physical Chemistry Chemical Physics **23**, 8336 (2021).
- [29] A. Loew, H.-C. Wang, T. F. Cerqueira, and M. A. Marques, Machine Learning: Science and Technology **5**, 045019 (2024).
- [30] S. Fang, M. Geiger, J. G. Checkelsky, and T. Smidt, “Phonon predictions with E(3)-equivariant graph neural networks,” (2024), arXiv:2403.11347 [cond-mat].
- [31] L. Fu, M. Kornbluth, Z. Cheng, and C. A. Marianetti, Physical Review B **100**, 014303 (2019).
- [32] D. H. Hurley, A. El-Azab, M. S. Bryan, M. W. D. Cooper, C. A. Dennett, K. Gofryk, L. He, M. Khafizov, G. H. Lander, M. E. Manley, J. M. Mann, C. A. Marianetti, K. Rickert, F. A. Selim, M. R. Tonks, and J. P. Wharry, Chemical Reviews **122**, 3711 (2022), pMID: 34919381.
- [33] M. Jin, C. Jiang, J. Gan, and D. H. Hurley, Journal of Nuclear Materials **536**, 152144 (2020).
- [34] C. A. Dennett, W. R. Deskins, M. Khafizov, Z. Hua, A. Khanolkar, K. Bawane, L. Fu, J. M. Mann, C. A. Marianetti, L. He, D. H. Hurley, and A. El-Azab, Acta

- Materialia **213**, 116934 (2021).
- [35] L. He, M. Khafizov, C. Jiang, B. Tyburska-Püschel, B. J. Jaques, P. Xiu, P. Xu, M. K. Meyer, K. Sridharan, D. P. Butt, and J. Gan, *Acta Materialia* **208**, 116778 (2021).
- [36] M. Khafizov, J. Pakarinen, L. He, and D. H. Hurley, *Journal of the American Ceramic Society* **102**, 7533 (2019).
- [37] M. Khafizov, M. F. Riyad, Y. Wang, J. Pakarinen, L. He, T. Yao, A. El-Azab, and D. Hurley, *Acta Materialia* **193**, 61 (2020).
- [38] W. R. Deskins, A. Khanolkar, S. Mazumder, C. A. Dennett, K. Bawane, Z. Hua, J. Ferrigno, L. He, J. M. Mann, M. Khafizov, *et al.*, *Acta Materialia* **241**, 118379 (2022).
- [39] M. Jin, J. Miao, Y. Zhang, M. Khafizov, K. K. Bawane, B. Kombaiyah, Y. Zhang, and D. H. Hurley, *Scripta Materialia* **237**, 115706 (2023).
- [40] L.-C. Yu, S. Zhou, M. Jin, M. Khafizov, D. Hurley, and Y. Zhang, *Nuclear Materials and Energy* **41**, 101774 (2024).
- [41] W. D. Neilson, C. O. Galvin, S. J. Dillon, M. W. Cooper, and D. A. Andersson, *Physical Review Materials* **8**, 103602 (2024).
- [42] W. D. Neilson, J. Rizk, M. W. Cooper, and D. A. Andersson, *The Journal of Physical Chemistry C* **128**, 21559 (2024).
- [43] L. Malakkal, A. Katre, S. Zhou, C. Jiang, D. H. Hurley, C. A. Marianetti, and M. Khafizov, *Physical Review Materials* **8**, 025401 (2024).
- [44] C. Jiang, C. A. Marianetti, M. Khafizov, and D. H. Hurley, *npj Computational Materials* **10**, 21 (2024).
- [45] X.-Y. Liu, M. W. D. Cooper, K. J. McClellan, J. C. Lashley, D. D. Byler, B. Bell, R. Grimes, C. R. Stanek, and D. A. Andersson, *Physical Review Applied* **6**, 044015 (2016).
- [46] J. Park, E. B. Farfán, K. Mitchell, A. Resnick, C. Enriquez, and T. Yee, *Journal of Nuclear Materials* **504**, 198 (2018).
- [47] M. W. D. Cooper, S. C. Middleburgh, and R. W. Grimes, *Journal of Nuclear Materials* **466**, 29 (2015).
- [48] J. Park, E. B. Farfán, and C. Enriquez, *Nuclear Engineering and Technology* **50**, 731 (2018).
- [49] H. Balboa, L. Van Brutzel, A. Chartier, and Y. Le Bouar, *Journal of Nuclear Materials* **495**, 67 (2017).
- [50] L. Malakkal, A. Prasad, E. Jossou, J. Ranasinghe, B. Szpunar, L. Bichler, and J. Szpunar, *Journal of Alloys and Compounds* **798**, 507 (2019).
- [51] X. Zhu, H. Gong, Y.-F. Zhao, D.-Y. Lin, G. Han, T. Liu, and H. Song, *Journal of Nuclear Materials* **533**, 152080 (2020).
- [52] C. Jiang, L. He, C. A. Dennett, M. Khafizov, J. M. Mann, and D. H. Hurley, *Scripta Materialia* **214**, 114684 (2022).
- [53] M. Jin, J. Miao, B. Chen, M. Khafizov, Y. Zhang, and D. H. Hurley, *Computational Materials Science* **235**, 112842 (2024).
- [54] P. C. Fossati, P. A. Burr, M. W. Cooper, C. O. Galvin, and R. W. Grimes, *Physical Review Materials* **8**, 115404 (2024).
- [55] M. Cooper, C. Matthews, and D. Andersson, *Journal of Nuclear Materials* **604**, 155452 (2025).
- [56] M. Jin, M. Khafizov, C. Jiang, S. Zhou, C. A. Marianetti, M. S. Bryan, M. E. Manley, and D. H. Hurley, *Journal of Physics: Condensed Matter* **33**, 275402 (2021).
- [57] M. A. Mathis, A. Khanolkar, L. Fu, M. S. Bryan, C. A. Dennett, K. Rickert, J. M. Mann, B. Winn, D. L. Abernathy, M. E. Manley, D. H. Hurley, and C. A. Marianetti, *Physical Review B* **106**, 014314 (2022).
- [58] E. Xiao, H. Ma, M. S. Bryan, L. Fu, J. M. Mann, B. Winn, D. L. Abernathy, R. P. Hermann, A. R. Khanolkar, C. A. Dennett, D. H. Hurley, M. E. Manley, and C. A. Marianetti, *Physical Review B* **106**, 144310 (2022).
- [59] S. Zhou, H. Ma, E. Xiao, K. Gofryk, C. Jiang, M. E. Manley, D. H. Hurley, and C. A. Marianetti, *Physical Review B* **106**, 125134 (2022).
- [60] S. Zhou, E. Xiao, H. Ma, K. Gofryk, C. Jiang, M. E. Manley, D. H. Hurley, and C. A. Marianetti, *Physical Review Letters* **132**, 106502 (2024), publisher: American Physical Society.
- [61] R. A. Buckingham and J. E. Lennard-Jones, *Proceedings of the Royal Society of London. Series A. Mathematical and Physical Sciences* **168**, 264 (1938).
- [62] P. M. Morse, *Physical Review* **34**, 57 (1929).
- [63] P. J. Mitchell and D. Fincham, **5**, 1031 (1993).
- [64] J. D. Gale, *Journal of the Chemical Society, Faraday Transactions* **93**, 629 (1997), publisher: The Royal Society of Chemistry.
- [65] See Supplemental Material at [link] for details of the training and assessment data, the training method for empirical potential, the training results for alternative analytical forms, the configurations of Frenkel pairs, the analyses and comparisons of second- and third-order irreducible derivatives, and the reciprocal coordinates of primary q points and their displacement bases. See also Ref. [90].
- [66] P. E. Blöchl, *Physical Review B* **50**, 17953 (1994).
- [67] G. Kresse and D. Joubert, *Physical Review B* **59**, 1758 (1999).
- [68] G. Kresse and J. Hafner, *Physical Review B* **47**, 558 (1993).
- [69] G. Kresse and J. Furthmüller, *Physical Review B* **54**, 11169 (1996).
- [70] J. Sun, A. Ruzsinszky, and J. P. Perdew, *Physical Review Letters* **115**, 036402 (2015).
- [71] J. P. Perdew, K. Burke, and M. Ernzerhof, *Physical Review Letters* **77**, 3865 (1996).
- [72] P. Maldonado, L. Paolasini, P. Oppeneer, T. R. Forrest, A. Prodi, N. Magnani, A. Bosak, G. Lander, and R. Caciuffo, *Physical Review B* **93**, 144301 (2016).
- [73] V. I. Anisimov, J. Zaanen, and O. K. Andersen, *Physical Review B* **44**, 943 (1991).
- [74] S. L. Dudarev, D. N. Manh, and A. P. Sutton, *Philosophical Magazine B* **75**, 613 (1997).
- [75] H. J. Monkhorst and J. D. Pack, *Physical Review B* **13**, 5188 (1976).
- [76] P. P. Ewald, *Annalen der Physik* **369**, 253 (1921).
- [77] M. J. Rushton, “potential-pro-fit,” <https://github.com/mjdrushton/potential-pro-fit>.
- [78] M. S. Bryan, J. W. L. Pang, B. C. Larson, A. Chernatynskiy, D. L. Abernathy, K. Gofryk, and M. E. Manley, *Physical Review Materials* **3**, 065405 (2019).
- [79] J. W. L. Pang, W. J. L. Buyers, A. Chernatynskiy, M. D. Lumsden, B. C. Larson, and S. R. Phillpot, *Physical Review Letters* **110**, 157401 (2013).
- [80] P. M. Macedo, W. Capps, and J. O. Wachtman, *Journal of the American Ceramic Society* **47**, 651 (1964).

- [81] A. Khanolkar, Y. Wang, C. A. Dennett, Z. Hua, J. M. Mann, M. Khafizov, and D. H. Hurley, *Journal of Applied Physics* **133**, 195101 (2023).
- [82] O. G. Brandt and C. T. Walker, *Physical Review Letters* **18**, 11 (1967).
- [83] H. Muta, Y. Murakami, M. Uno, K. Kurosaki, and S. Yamanaka, *Journal of Nuclear Science and Technology* **50**, 181 (2013).
- [84] K. Bakker, E. H. P. Cordfunke, R. J. M. Konings, and R. P. C. Schram, *Journal of Nuclear Materials* **250**, 1 (1997).
- [85] J. K. Fink, *Journal of Nuclear Materials* **279**, 1 (2000).
- [86] J. L. Bates, *Nuclear Science and Engineering* **21**, 26 (1965).
- [87] T. G. Godfrey, W. Fulkerson, T. G. Kollie, J. P. Moore, and D. L. McELROY, *Journal of the American Ceramic Society* **48**, 297 (1965).
- [88] C. Ronchi, M. Sheindlin, D. Staicu, and M. Kinoshita, *Journal of Nuclear Materials* **327**, 58 (2004).
- [89] K. Hirata, K. Moriya, and Y. Waseda, *Journal of Materials Science* **12**, 838 (1977).
- [90] K. Momma and F. Izumi, *Journal of Applied Crystallography* **44**, 1272 (2011).

Supplemental materials to

Parameterizing empirical interatomic potentials for predicting thermophysical properties via an irreducible derivative approach: the case of ThO₂ and UO₂

Shuxiang Zhou¹, Chao Jiang¹, Enda Xiao², Sasaank Bandi³, Michael W.D. Cooper⁴,
Miaomiao Jin⁵, David H Hurley¹, Marat Khafizov⁶, and Chris A. Marianetti³

¹*Idaho National Laboratory, Idaho Falls, ID 83415, USA*

²*Department of Chemistry, Columbia University, New York, NY 10027, USA*

³*Department of Applied Physics and Applied Mathematics,
Columbia University, New York, NY 10027, USA*

⁴*Los Alamos National Laboratory, Los Alamos, NM 87545, USA*

⁵*Department of Nuclear Engineering, The Pennsylvania State University, University Park, PA 16802, USA*

⁶*Department of Mechanical and Aerospace Engineering,
The Ohio State University, Columbus, OH 43210, USA*

I. PROPERTIES IN THE TRAINING PROCEDURE AND MODEL ASSESSMENT

TABLE S1. Summary of DFT-calculated properties in the training and assessment.

Property	Training data			Assessment data	
	Data	Weight	See in	Data	See in
Lattice parameter at $T = 0$, $a(0)$	All data	3700	Table III		
Normalized Born effective charge Z_{α}^*	All data	3700	Table III		
Frenkel pair (FP) formation energy E_F	a Th or U FP in the supercell $\hat{\mathbf{S}}_C$	20	Table III	a Th or U FP and two O FPs in the supercell $2\hat{\mathbf{S}}_C$	Table IV
Strain IDs $d_{\alpha_1\alpha_2}$	All data	55	Table III		
Second-order IDs $d_{q_1q_2}^{\alpha_1\alpha_2}$	within the supercell $2\hat{\mathbf{S}}_I$	75	Table III and Figure S2 S3	within the supercell $4\hat{\mathbf{S}}_I$, excluding the training data	Figure S2 S3
Third-order IDs $d_{q_1q_2q_3}^{\alpha_1\alpha_2\alpha_3}$	within the supercell $\hat{\mathbf{S}}_C$	37	Table S2 and Figure S2 S3	within the supercell $\hat{\mathbf{S}}_O$, excluding the training data	Figure S2 S3
Phonon dispersion				All data	Figure 1
Thermal conductivity				All data	Figure 2

ThO₂ and UO₂ have a face-centered cubic lattice; the lattice vectors chosen are given in a row-stacked matrix:

$$\hat{\mathbf{a}} = \frac{a}{2} \begin{bmatrix} 0 & 1 & 1 \\ 1 & 0 & 1 \\ 1 & 1 & 0 \end{bmatrix}, \quad (1)$$

where a is the lattice parameter of a conventional cubic cell. There are three classes of supercells used to define the discretization of the phonon interactions: $n\hat{\mathbf{S}}_I = n\hat{\mathbf{1}}$ (i.e., uniform supercells), $n\hat{\mathbf{S}}_C = n(\hat{\mathbf{J}} - 2\hat{\mathbf{1}})$, and $n\hat{\mathbf{S}}_O = n(4\hat{\mathbf{1}} - \hat{\mathbf{J}})$, where n is a positive integer, $\hat{\mathbf{1}}$ is the 3×3 identity matrix, and $\hat{\mathbf{J}}$ is a 3×3 matrix with each element being 1. The crystal structures used for FPs are given in Section IV of SM.

II. METHOD FOR TRAINING THE EMPIRICAL POTENTIAL

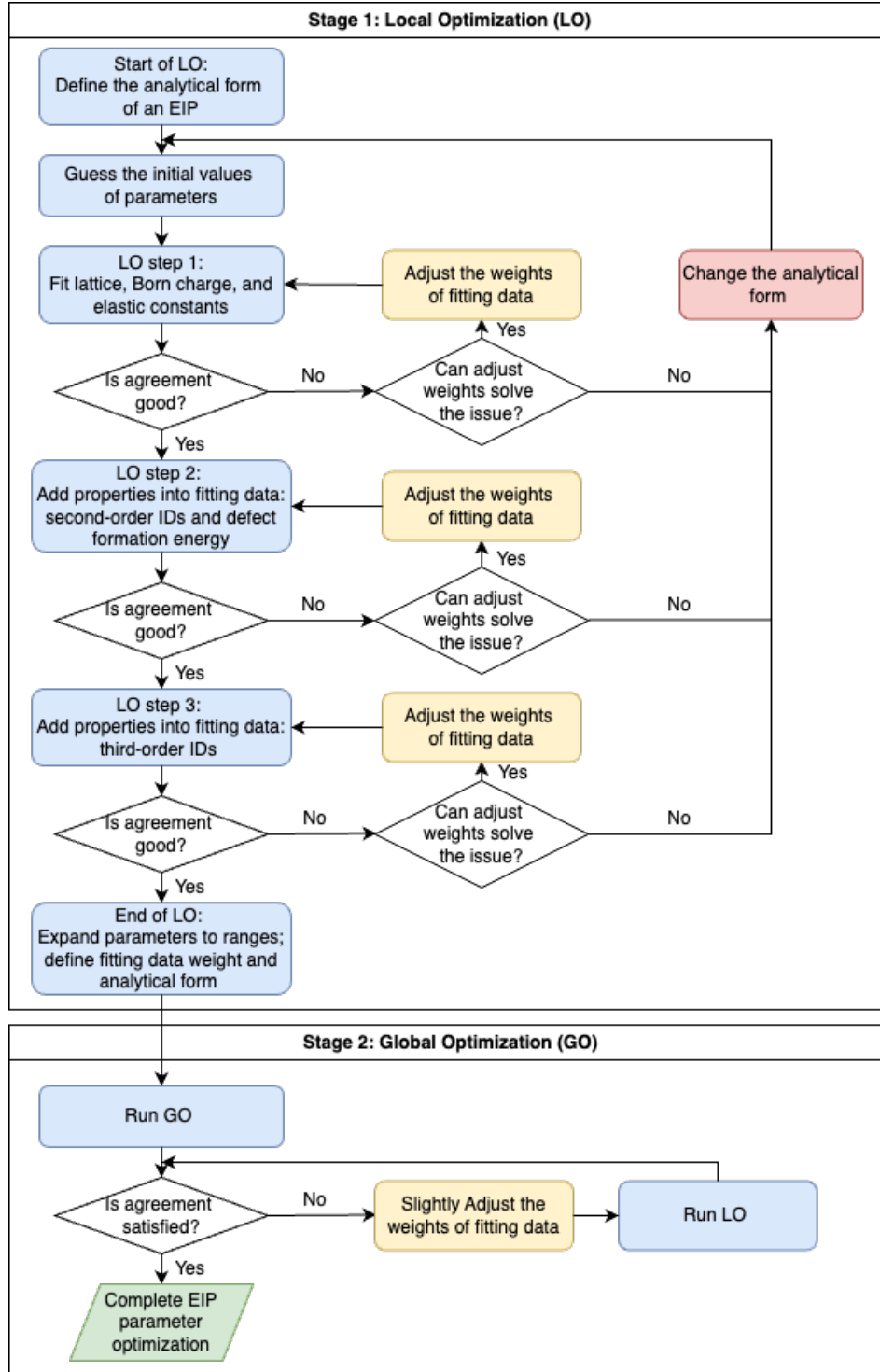


FIG. S1. Flowchart of parameter optimization for EIP training in this work.

Here we provide the method for the parameter optimization of EIP training in this work, where a two-stage approach is developed (see the flowchart in Figure S1). The challenge of parameter optimization of EIP results from all the variables, including the analytical form of EIP, the range of parameters, and the training data set and its weight. If all this information is already known, one can use a given global optimization (GO) algorithm, e.g., the particle

swarm algorithm as applied in this work, and complete the parameter optimization process in one shot. Therefore, in our two-stage approach, the main target of Stage 1 is to obtain the aforementioned information for variables by applying local optimization (LO) algorithms, e.g., the Nelder–Mead method as applied in this work, then run GO in Stage 2. Stage 1 starts by defining the analytical form of an EIP and the initial values of parameters, and the existing EIPs for the same material or similar systems can be valuable references. Then we add the training data into LO step by step, generally in the order from basic properties to complex properties. To improve the predictions of phonon properties, we designed three steps: first, the training data containing the lattice, elastic constants, and the effective Born charge; secondly, the second-order IDs and defect formation energy are added to the training data; then finally, the third-order IDs are added. In each step, the weights of training data are adjusted, so that a reasonable agreement is obtained. If some issues cannot be fixed by adjusting the weights of training data, these issues are likely due to the analytical form of the EIP. For example, the phonon energies of the highest two optical branches are always approximately identical without the core-shell model for ThO_2 , thus we add the core-shell model for improvement.

After Stage 1, the range of each parameter can be estimated by expanding its value, e.g., by 2 times or 10 times, depending on the computational resources available for GO. With the analytical form and the training data set and its weight defined in Stage 1, one can start Stage 2 of GO. After GO, if small improvements are required, one can always slightly adjust the weights and re-run LO. Finally, the EIP parameter optimization process is completed.

III. COMPARISON OF DISPLACEMENT IRREDUCIBLE DERIVATIVES

We compare the second- and third-order displacement irreducible derivatives computed from EIPs (the CRG and the PW) and DFT, for both ThO_2 (see Figure S2) and UO_2 (see Figure S3). Please note that the training and assessment data are according to the PW, as the CRG was not trained based on DFT data. The second- and third-order displacement irreducible derivatives are computed using the CRG for the sake of comparison.

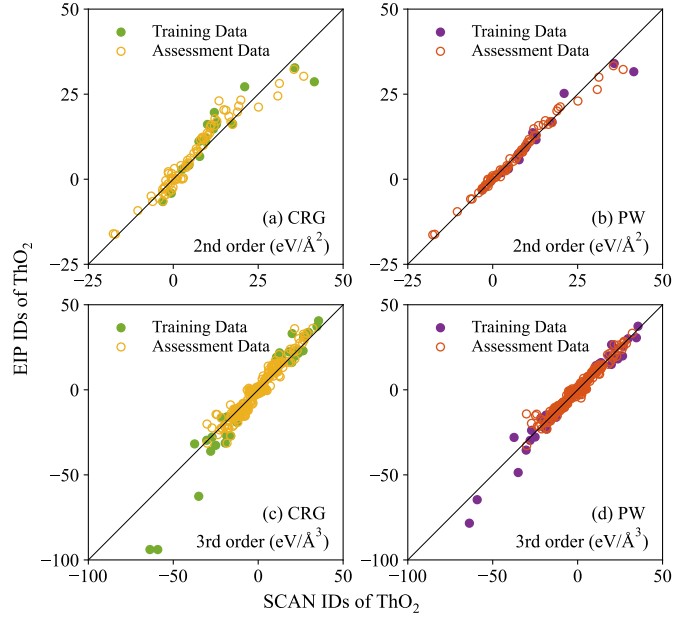


FIG. S2. Comparison of computed second- and third-order displacement irreducible derivatives between EIPs (the CRG and the PW) and SCAN for ThO_2 . Only solid dots were used in the potential training process.

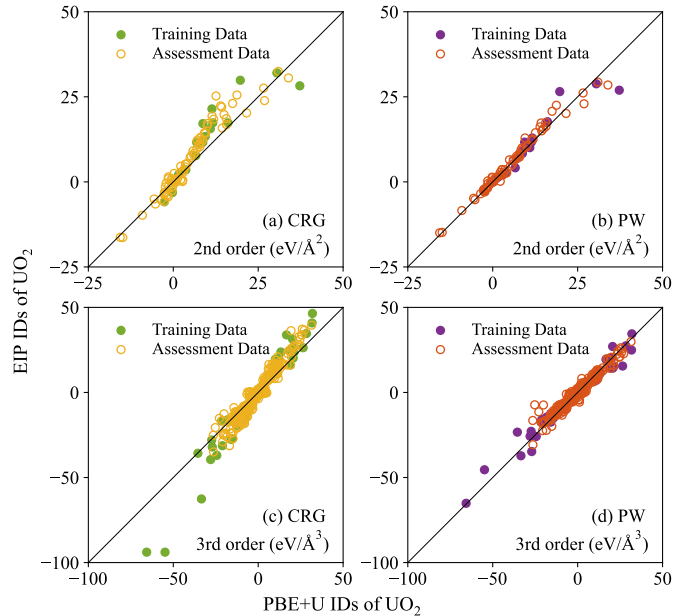
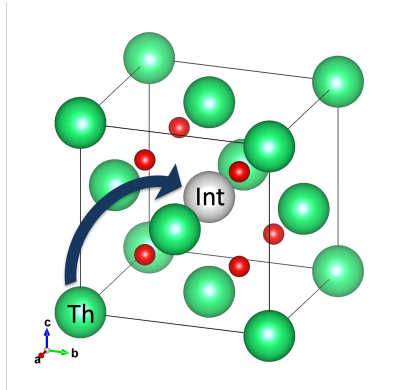


FIG. S3. Comparison of computed second- and third-order displacement irreducible derivatives between EIPs (the CRG and the PW) and PBE+ U for UO_2 . Only solid dots were used in the potential training process.

IV. THE CONFIGURATION OF FRENKEL PAIRS

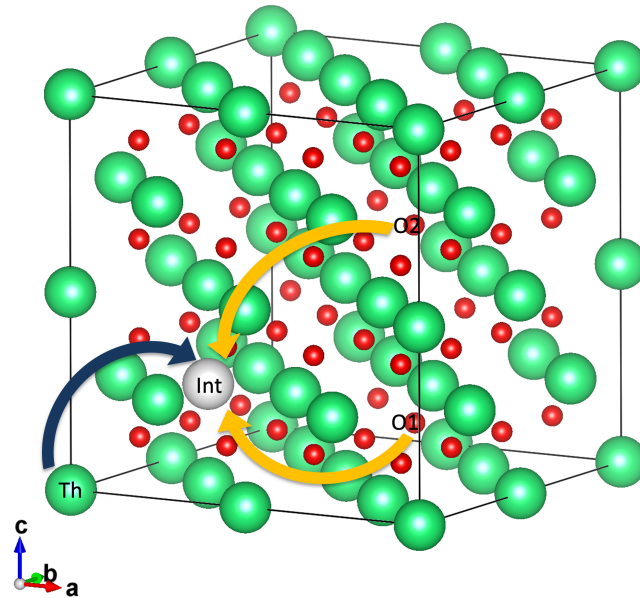
The training set contains two data points: Th (or U) FP in the conventional cubic supercell (\hat{S}_C).

- Th (or U) FP: the Th (or U) atom at $(0, 0, 0)$ is moved to the octahedral interstitial site at $(0.5, 0.5, 0.5)$.



The assessment set contains six data points: one Th (or U) FP and two O FPs in the $2 \times 2 \times 2$ conventional cubic supercell ($2\hat{S}_C$).

- Th (or U) FP: the Th (or U) atom at $(0, 0, 0)$ is moved to the octahedral interstitial site at $(0.25, 0.25, 0.25)$.
- O FP1: the O atom at $(0.675, 0.675, 0.125)$ is moved to the octahedral interstitial site at $(0.25, 0.25, 0.25)$.
- O FP2: the O atom at $(0.675, 0.675, 0.675)$ is moved to the octahedral interstitial site at $(0.25, 0.25, 0.25)$.



The crystal structure is visualized by the VESTA package [1].

V. TRAINING DATA OF THIRD-ORDER IRREDUCIBLE DERIVATIVES

TABLE S2. The third-order displacement IDs in the training data computed by DFT, and compared with the CRG and the PW.

Property	ThO ₂			UO ₂		
	SCAN	CRG	PW	PBE+ <i>U</i>	CRG	PW
Third-order irreducible derivatives within the conventional cubic supercell (eV/Å ³)						
$d_{\Gamma\Gamma\Gamma}^{T_{2g}T_{2g}T_{2g}}$	-63.74	-93.90	-78.41	-65.66	-93.88	-65.15
$d_{\Gamma\Gamma\Gamma}^{T_{1u}T_{1u}T_{2g}}$	-59.14	-93.90	-64.60	-54.86	-93.89	-45.44
$d_{\Gamma XX}^{T_{2g}A_{1g}E_g}$	-18.55	-16.06	-14.97	-18.12	-16.13	-14.48
$d_{\Gamma XX}^{T_{1u}A_{1g}{}^2A_{2u}}$	35.55	40.55	37.38	31.93	46.45	34.46
$d_{\Gamma XX}^{T_{1u}A_{1g}E_u}$	-27.12	-27.82	-23.81	-27.37	-27.93	-22.86
$d_{\Gamma XX}^{T_{1u}A_{1g}{}^1E_u}$	29.66	33.78	30.02	28.39	34.64	27.40
$d_{\Gamma XX}^{T_{2g}E_gE_g}$	26.69	31.30	25.50	20.26	31.30	20.53
$d_{\Gamma XX}^{T_{1u}E_g{}^2A_{2u}}$	34.58	37.22	30.60	31.72	40.84	24.93
$d_{\Gamma XX}^{T_{1u}B_{1u}E_g}$	-18.40	-27.11	-19.78	-15.09	-27.10	-14.48
$d_{\Gamma XX}^{T_{1u}E_gE_u}$	-16.17	-27.11	-18.33	-15.83	-27.10	-12.41
$d_{\Gamma XX}^{T_{1u}E_g{}^1E_u}$	19.98	33.07	26.54	16.67	33.82	19.43
$d_{\Gamma XX}^{T_{2g}B_{1u}{}^2A_{2u}}$	26.42	22.94	19.88	26.47	26.29	15.53
$d_{\Gamma XX}^{T_{2g}{}^2A_{2u}E_u}$	12.57	21.73	15.18	13.36	23.78	11.35
$d_{\Gamma XX}^{T_{2g}{}^2A_{2u}{}^1E_u}$	-27.96	-36.11	-29.74	-27.99	-39.44	-25.74
$d_{\Gamma XX}^{T_{2g}B_{1u}E_u}$	-11.66	-15.65	-11.91	-10.42	-15.65	-9.13
$d_{\Gamma XX}^{T_{2g}B_{1u}{}^1E_u}$	13.78	19.09	15.99	12.29	19.52	12.34
$d_{\Gamma XX}^{T_{2g}E_uE_u}$	-19.42	-31.30	-22.45	-21.05	-31.29	-15.90
$d_{\Gamma XX}^{T_{2g}E_u{}^1E_u}$	10.90	19.09	11.98	10.84	19.52	7.07
$d_{\Gamma XX}^{T_{2g}{}^1E_u{}^1E_u}$	-35.01	-62.60	-48.62	-33.40	-62.59	-37.23
$d_{X_2X_1X}^{A_{1g}A_{1g}A_{1g}}$	-21.61	-16.56	-16.57	-21.57	-16.81	-17.44
$d_{X_2X_1X}^{A_{1g}E_gE_g}$	19.83	16.06	14.90	18.94	16.13	14.35
$d_{X_2X_1X}^{A_{1g}{}^2A_{2u}E_u}$	18.20	22.34	19.88	18.64	24.49	19.38
$d_{X_2X_1X}^{A_{1g}{}^2A_{2u}{}^1E_u}$	-25.04	-32.63	-27.74	-24.38	-36.98	-25.87
$d_{X_2X_1X}^{A_{1g}B_{1u}B_{1u}}$	-18.46	-16.06	-14.88	-16.92	-16.13	-14.32
$d_{X_2X_1X}^{A_{1g}E_uE_u}$	-13.73	-16.06	-14.60	-14.28	-16.13	-15.08
$d_{X_2X_1X}^{A_{1g}E_u{}^1E_u}$	21.57	19.67	24.72	20.60	20.20	27.01
$d_{X_2X_1X}^{A_{1g}{}^1E_u{}^1E_u}$	-30.31	-29.67	-35.45	-27.04	-32.06	-34.74
$d_{X_2X_1X}^{E_gE_gE_g}$	-11.65	-15.65	-12.58	-7.96	-15.65	-9.95
$d_{X_2X_1X}^{E_g{}^2A_{2u}B_{1u}}$	23.59	21.47	18.14	21.10	23.56	14.99
$d_{X_2X_1X}^{E_gB_{1u}E_u}$	11.48	15.65	11.57	9.99	15.65	8.56
$d_{X_2X_1X}^{E_gB_{1u}{}^1E_u}$	-12.64	-19.09	-16.12	-11.73	-19.52	-12.29
$d_{X_2X_1X}^{E_gE_u{}^2A_{2u}}$	22.21	22.97	18.67	20.60	26.31	14.26
$d_{X_2X_1X}^{E_gE_uE_u}$	-10.36	-15.65	-10.85	-10.17	-15.65	-7.43
$d_{X_2X_1X}^{E_gE_u{}^1E_u}$	10.80	19.09	14.21	10.10	19.52	9.85
${}^1d_{X_2X_1X}^{E_gE_u{}^1E_u}$	12.28	19.09	14.21	11.51	19.52	9.85
$d_{X_2X_1X}^{E_g{}^1E_u{}^2A_{2u}}$	-37.43	-31.81	-28.00	-35.49	-35.75	-23.34
$d_{X_2X_1X}^{E_g{}^1E_u{}^1E_u}$	-18.46	-27.00	-23.08	-15.83	-27.61	-17.45

VI. THE SPECTRAL AND CUMULATIVE THERMAL CONDUCTIVITY

In this section, we report the calculated spectral and cumulative thermal conductivity as functions of phonon energy at $T = 1000$ K obtained from BTE-RTA calculations, shown in Fig. S4. The black dashed lines, denoted as *exp*, represent the mean values of linearly interpolated experimental data for ThO_2 [2, 3] and UO_2 [4–7] at $T = 1000$ K, respectively. For both the DFT and the PW results, the highest optical phonon mode, where the phonon energy > 65 meV and 62 meV for ThO_2 and UO_2 , respectively, has a thermal conductivity contribution $< 3\%$.

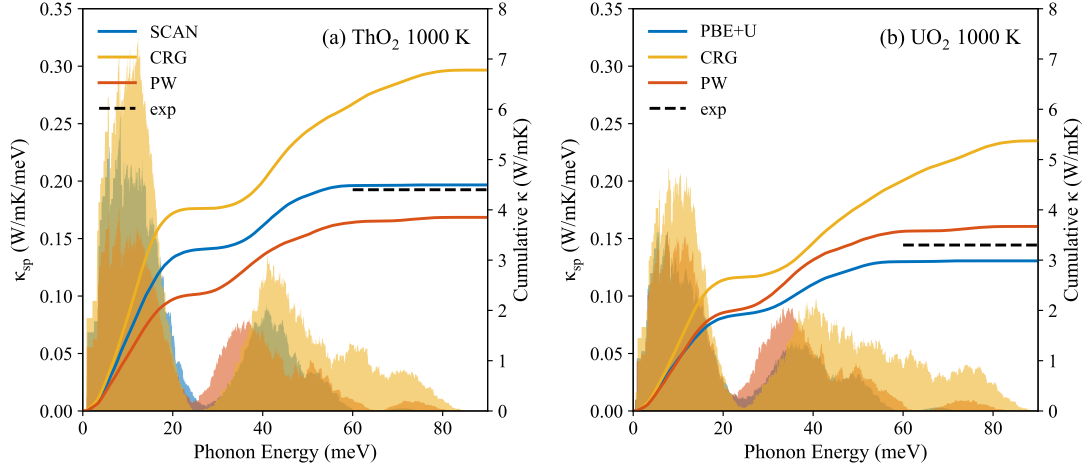


FIG. S4. Calculated spectral and cumulative thermal conductivity as functions of phonon energy at $T = 1000$ K obtained from the BTE within the RTA for (a) ThO_2 and (b) UO_2 , using DFT, the CRG, and the PW. The black dashed lines, denoted as *exp*, represent the mean values of linearly interpolated experimental data for ThO_2 [2, 3] and UO_2 [4–7] at $T = 1000$ K, respectively.

VII. ALTERNATIVE ANALYTICAL FORMS

The analytical functional form of our EIP in the main text contains three portions (pairwise potentials, many-body potentials, and the core-shell model), here we benchmark two alternative analytical forms: (1) only pairwise potentials, denoted as PW_pair; (2) pairwise potentials plus many-body potentials of EAM, denoted as PW_eam. PW_eam is in the same form as the CRG potential. PW_pair and PW_eam were trained using the method provided in Section II of SM, and their parameter values and the computed properties are presented in this section.

Note that, in an EAM potential without the core-shell model, for each element, the normalized Born effective charge is equal to the charge ($Z_\alpha^* = q_\alpha$). As $q_{Th} = q_U = -2q_O$, we have a constraint of $Z_{Th}^* = Z_U^*$. However, Z_{Th}^* and Z_U^* are different when computed within DFT (as $Z_{Th}^* = 2.448|e|$, $Z_U^* = 2.325|e|$). Therefore, the values of Z_{Th}^* and Z_U^* in EIP should be the mean value of Z_{Th}^* and Z_U^* from DFT; we obtained $q_{Th} = q_U = 2.3865|e|$ and $q_O = -1.19325|e|$, for both PW_pair and PW_eam.

Both PW_pair and PW_eam models are simpler than the PW, and thus inevitably, they have larger overall errors than the PW, as well as some other limitations. For PW_pair, we observed two major errors: the highest two optical branches are nearly degenerate at the L point, and $C_{12} \approx C_{44}$. While the many-body potential differentiates C_{12} and C_{44} in PW_eam, the highest two optical branches are still approximately degenerate at the L point, as only a small gap is observed. The core-shell model, as shown in the PW, can overcome this limitation of nearly degenerate optical modes at the L point, while improving the thermal expansion prediction.

TABLE S3. Parameters of PW_pair for the short-range pairwise potentials.

Interaction	$\phi_B(r_{ij})$			$\phi_M(r_{ij})$		
	$A_{\alpha\beta}(eV)$	$\rho_{\alpha\beta}(\text{\AA})$	$C_{\alpha\beta}(eV\text{\AA}^6)$	$D_{\alpha\beta}(eV)$	$\gamma_{\alpha\beta}(\text{\AA}^{-1})$	$r_0(\text{\AA})$
Th-Th	33 435.38	0.3189	2.0174	10.9021	6.7716	2.5580
U-U	32 188.29	0.3142	2.0017	11.0094	6.7674	2.5421
Th-O	184.81	0.4286	10.2301	0.4770	2.2433	2.3957
U-O	190.91	0.4278	9.8838	0.4678	2.1416	2.3639
O-O	813.34	0.3264	0.4932	-	-	-

TABLE S4. Parameters of PW_eam for the short-range pairwise potentials.

Interaction	$\phi_B(r_{ij})$			$\phi_M(r_{ij})$		
	$A_{\alpha\beta}(eV)$	$\rho_{\alpha\beta}(\text{\AA})$	$C_{\alpha\beta}(eV\text{\AA}^6)$	$D_{\alpha\beta}(eV)$	$\gamma_{\alpha\beta}(\text{\AA}^{-1})$	$r_0(\text{\AA})$
Th-Th	41 277.44	0.3107	4.2405	11.2342	7.6147	2.5705
U-U	39 471.38	0.3087	4.6978	10.8305	7.7293	2.5609
Th-O	305.57	0.4160	6.8704	0.4342	2.2179	2.4731
U-O	305.72	0.4194	5.5307	0.4496	2.2057	2.4315
O-O	630.18	0.3461	0.8693	-	-	-

TABLE S5. Parameters of PW_eam for many-body interactions and the Coulomb potential. The charge values (q) of PW_eam are as same as PW_pair.

Species	$G_\alpha(eV\text{\AA}^{1.5})$	$n_\alpha(\text{\AA}^5)$	$q_\alpha(e)$
Th	2.4472	1173.44	2.386 50
U	2.6547	1151.67	2.386 50
O	0.4619	252.07	-1.193 25

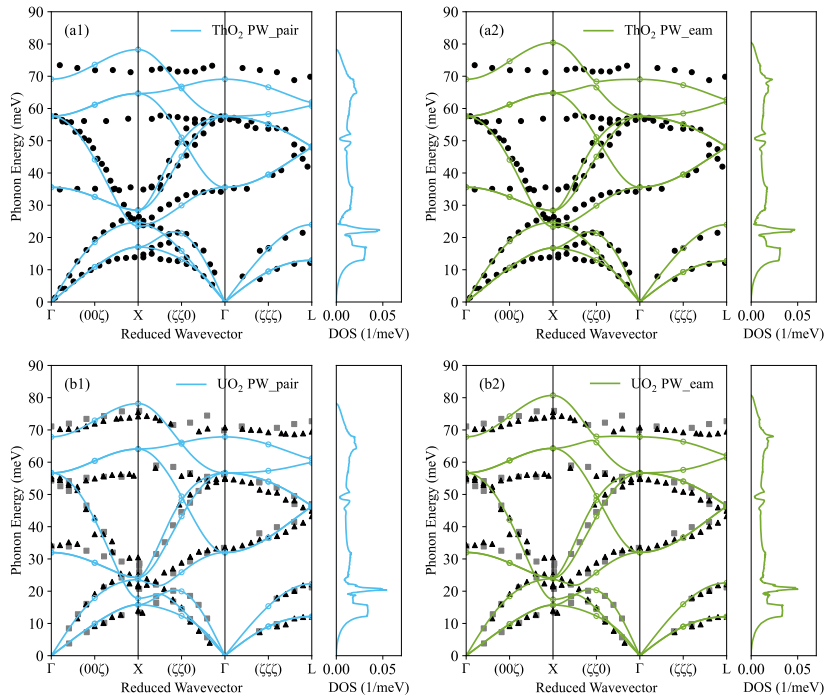


FIG. S5. Calculated phonon dispersion and density of states for (a) ThO_2 and (b) UO_2 , using (1) PW_pair and (2) PW_eam, compared to experimental data.

TABLE S6. Elastic constants and defect formation energy E_F for FPs calculated using DFT, the PW_pair, and the PW_eam in comparison to experimental data.

Property	ThO_2				UO_2			
	SCAN	PW_pair	PW_eam	exp	PBE+U	PW_pair	PW_eam	exp
Lattice constant at $T = 0$ K (\AA)								
$a(0)$	5.594	5.590	5.594		5.546	5.546	5.546	
Elastic constants (GPa)								
C_{11}	376	350	375	$367^a, 366^b$	380	343	380	400^c
C_{12}	117	96	127	$106^a, 114^b$	120	82	119	125^c
C_{44}	81	95	90	$80^a, 81^b$	63	82	80	59^c
Defect formation energy E_F (eV)								
O FP1	4.55	5.27	5.32		4.02	4.94	5.05	
O FP2	4.63	5.60	5.66		4.06	5.25	5.38	
Th or U FP	13.15	12.49	14.02		10.26	8.33	12.27	

^a Ref. [8], ^b Ref. [9], ^c Ref. [10].

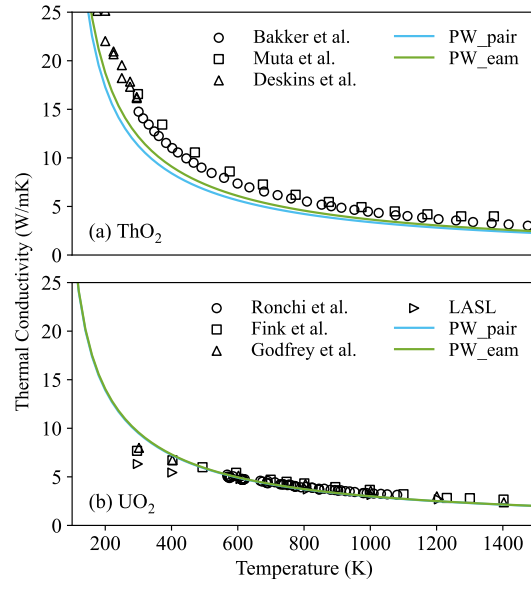


FIG. S6. Calculated phonon thermal conductivity of (a) ThO_2 and (b) UO_2 , using the PW_pair and the PW_eam at $T = 100 - 1500$ K, compared with the experimental data.

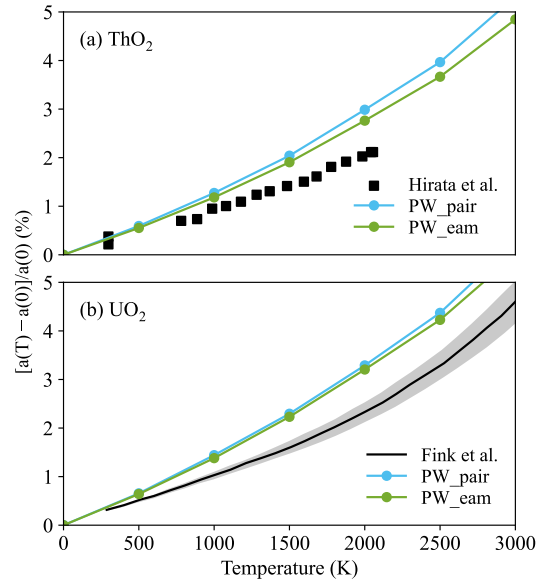


FIG. S7. Calculated percentage change of the lattice parameter as a function of temperature at $T = 0 - 3000$ K for (a) ThO_2 and (b) UO_2 , compared with the experiments.

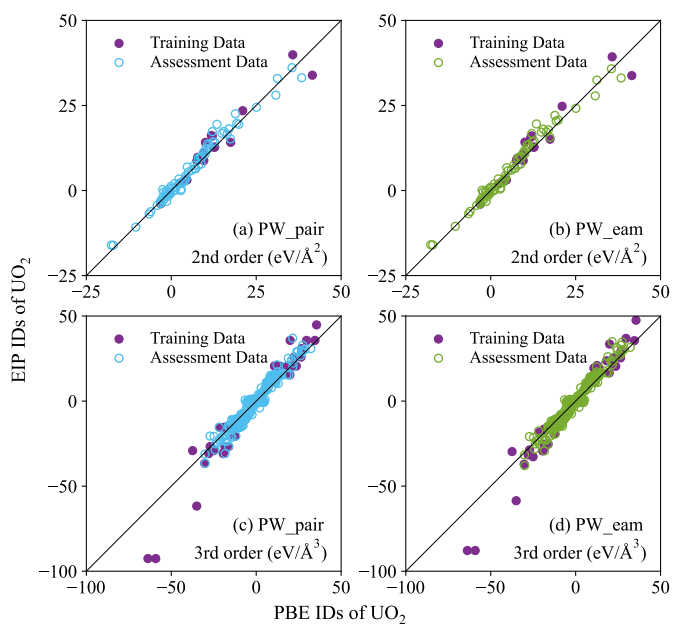


FIG. S8. Comparison of computed second- and third-order displacement irreducible derivatives between EIPs (the PW_pair and the PW_eam) and SCAN for ThO_2 . Only solid dots were used in the potential training process.

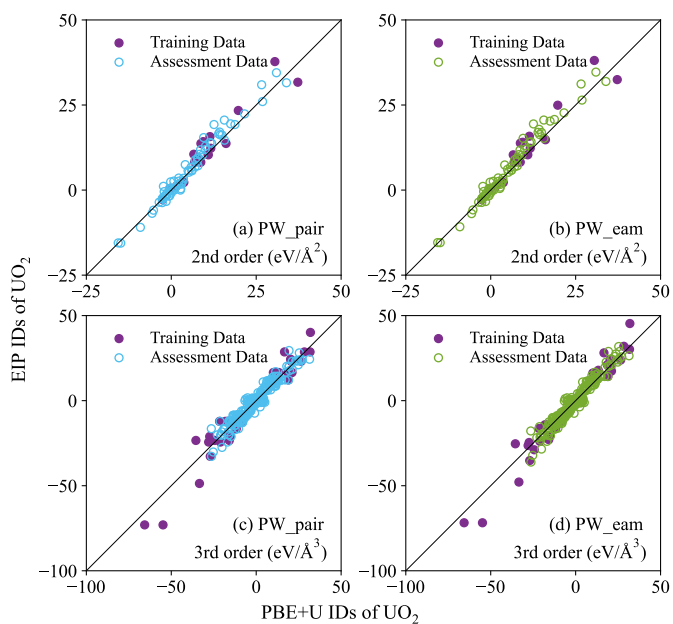


FIG. S9. Comparison of computed second- and third-order displacement irreducible derivatives between EIPs (the PW_pair and the PW_eam) and PBE+ U for UO_2 . Only solid dots were used in the potential training process.

VIII. PRIMARY \mathbf{q} POINTS AND SYMMETRIZED ATOMIC DISPLACEMENT BASIS

The primary \mathbf{q} points for ThO_2 or UO_2 are listed in Eq. (2), and the symmetrized atomic displacement basis of the primary \mathbf{q} points are tabulated in Table S7.

$$\begin{aligned}
&\Gamma = (000) \\
&L = \begin{pmatrix} 1 & 0 & 0 \\ 2 & & \end{pmatrix} \quad L_1 = \begin{pmatrix} 1 & 1 & 1 \\ 2 & 2 & 2 \end{pmatrix} \quad L_2 = \begin{pmatrix} 0 & 1 & 0 \\ 2 & & \end{pmatrix} \quad L_3 = \begin{pmatrix} 0 & 0 & 1 \\ & & 2 \end{pmatrix} \\
&X = \begin{pmatrix} 1 & 1 \\ 2 & 2 \end{pmatrix} \begin{pmatrix} 0 \\ 2 \end{pmatrix} \quad X_1 = \begin{pmatrix} 0 & 1 & 1 \\ 2 & 2 & \end{pmatrix} \quad X_2 = \begin{pmatrix} 1 & 0 & 1 \\ 2 & & 2 \end{pmatrix} \\
&\Delta = \begin{pmatrix} 1 & 1 \\ 4 & 4 \end{pmatrix} \begin{pmatrix} 0 \\ 4 \end{pmatrix} \quad \bar{\Delta} = \begin{pmatrix} 3 & 3 \\ 4 & 4 \end{pmatrix} \begin{pmatrix} 0 \\ 4 \end{pmatrix} \quad \Delta_1 = \begin{pmatrix} 0 & 1 & 1 \\ 4 & 4 & \end{pmatrix} \quad \bar{\Delta}_1 = \begin{pmatrix} 0 & 3 & 3 \\ 4 & 4 & \end{pmatrix} \quad \Delta_2 = \begin{pmatrix} 3 & 0 & 3 \\ 4 & 4 & \end{pmatrix} \quad \bar{\Delta}_2 = \begin{pmatrix} 1 & 0 & 1 \\ 4 & 4 & \end{pmatrix} \\
&W = \begin{pmatrix} 1 & 3 & 1 \\ 4 & 4 & 2 \end{pmatrix} \begin{pmatrix} 0 \\ 4 \\ 2 \end{pmatrix} \quad \bar{W} = \begin{pmatrix} 3 & 1 & 1 \\ 4 & 4 & 2 \end{pmatrix} \begin{pmatrix} 0 \\ 4 \\ 2 \end{pmatrix} \quad W_1 = \begin{pmatrix} 1 & 1 & 3 \\ 2 & 4 & 4 \end{pmatrix} \begin{pmatrix} 0 \\ 2 \\ 4 \end{pmatrix} \quad \bar{W}_1 = \begin{pmatrix} 1 & 3 & 1 \\ 2 & 4 & 4 \end{pmatrix} \begin{pmatrix} 0 \\ 2 \\ 4 \end{pmatrix} \quad W_2 = \begin{pmatrix} 1 & 1 & 3 \\ 4 & 2 & 4 \end{pmatrix} \begin{pmatrix} 0 \\ 4 \\ 2 \end{pmatrix} \quad \bar{W}_2 = \begin{pmatrix} 3 & 1 & 1 \\ 4 & 2 & 4 \end{pmatrix} \begin{pmatrix} 0 \\ 4 \\ 2 \end{pmatrix} \\
&A = \begin{pmatrix} 1 & 3 \\ 4 & 4 \end{pmatrix} \begin{pmatrix} 0 \\ 4 \end{pmatrix} \quad \bar{A} = \begin{pmatrix} 3 & 1 \\ 4 & 4 \end{pmatrix} \begin{pmatrix} 0 \\ 4 \end{pmatrix} \quad A_1 = \begin{pmatrix} 1 & 3 & 3 \\ 2 & 4 & 4 \end{pmatrix} \begin{pmatrix} 0 \\ 2 \\ 4 \end{pmatrix} \quad \bar{A}_1 = \begin{pmatrix} 1 & 1 & 1 \\ 2 & 4 & 4 \end{pmatrix} \begin{pmatrix} 0 \\ 2 \\ 4 \end{pmatrix} \quad A_2 = \begin{pmatrix} 1 & 0 & 3 \\ 4 & 4 & \end{pmatrix} \begin{pmatrix} 0 \\ 4 \\ \end{pmatrix} \quad \bar{A}_2 = \begin{pmatrix} 3 & 0 & 1 \\ 4 & 4 & \end{pmatrix} \begin{pmatrix} 0 \\ 4 \\ \end{pmatrix} \\
&A_3 = \begin{pmatrix} 0 & 3 & 1 \\ 4 & 4 & \end{pmatrix} \begin{pmatrix} 0 \\ 4 \\ \end{pmatrix} \quad \bar{A}_3 = \begin{pmatrix} 0 & 1 & 3 \\ 4 & 4 & \end{pmatrix} \begin{pmatrix} 0 \\ 4 \\ \end{pmatrix} \quad A_4 = \begin{pmatrix} 3 & 1 & 3 \\ 4 & 2 & 4 \end{pmatrix} \begin{pmatrix} 0 \\ 2 \\ 4 \end{pmatrix} \quad \bar{A}_4 = \begin{pmatrix} 1 & 1 & 1 \\ 4 & 2 & 4 \end{pmatrix} \begin{pmatrix} 0 \\ 2 \\ 4 \end{pmatrix} \quad A_5 = \begin{pmatrix} 1 & 1 & 1 \\ 4 & 4 & 2 \end{pmatrix} \begin{pmatrix} 0 \\ 4 \\ 2 \end{pmatrix} \quad \bar{A}_5 = \begin{pmatrix} 3 & 3 & 1 \\ 4 & 4 & 2 \end{pmatrix} \begin{pmatrix} 0 \\ 4 \\ 2 \end{pmatrix} \\
&\Lambda = \begin{pmatrix} 1 & 0 & 0 \\ 4 & & \end{pmatrix} \begin{pmatrix} 0 \\ 4 \\ \end{pmatrix} \quad \bar{\Lambda} = \begin{pmatrix} 3 & 0 & 0 \\ 4 & & \end{pmatrix} \begin{pmatrix} 0 \\ 4 \\ \end{pmatrix} \quad \Lambda_1 = \begin{pmatrix} 0 & 3 & 0 \\ 4 & & \end{pmatrix} \begin{pmatrix} 0 \\ 4 \\ \end{pmatrix} \quad \bar{\Lambda}_1 = \begin{pmatrix} 0 & 1 & 0 \\ 4 & & \end{pmatrix} \begin{pmatrix} 0 \\ 4 \\ \end{pmatrix} \quad \Lambda_2 = \begin{pmatrix} 0 & 0 & 3 \\ 4 & & \end{pmatrix} \begin{pmatrix} 0 \\ 4 \\ \end{pmatrix} \quad \bar{\Lambda}_2 = \begin{pmatrix} 0 & 0 & 1 \\ 4 & & \end{pmatrix} \begin{pmatrix} 0 \\ 4 \\ \end{pmatrix} \\
&\Lambda_3 = \begin{pmatrix} 1 & 1 & 1 \\ 4 & 4 & 4 \end{pmatrix} \begin{pmatrix} 0 \\ 4 \\ 4 \end{pmatrix} \quad \bar{\Lambda}_3 = \begin{pmatrix} 3 & 3 & 3 \\ 4 & 4 & 4 \end{pmatrix} \begin{pmatrix} 0 \\ 4 \\ 4 \end{pmatrix} \\
&B = \begin{pmatrix} 1 & 1 \\ 4 & 2 \end{pmatrix} \begin{pmatrix} 0 \\ 4 \end{pmatrix} \quad \bar{B} = \begin{pmatrix} 3 & 1 \\ 4 & 2 \end{pmatrix} \begin{pmatrix} 0 \\ 4 \end{pmatrix} \quad B_1 = \begin{pmatrix} 1 & 3 & 1 \\ 2 & 4 & 2 \end{pmatrix} \begin{pmatrix} 0 \\ 2 \\ 4 \end{pmatrix} \quad \bar{B}_1 = \begin{pmatrix} 1 & 1 & 1 \\ 2 & 4 & 2 \end{pmatrix} \begin{pmatrix} 0 \\ 2 \\ 4 \end{pmatrix} \quad B_2 = \begin{pmatrix} 3 & 3 & 1 \\ 4 & 4 & 4 \end{pmatrix} \begin{pmatrix} 0 \\ 4 \\ 4 \end{pmatrix} \quad \bar{B}_2 = \begin{pmatrix} 1 & 1 & 3 \\ 4 & 4 & 4 \end{pmatrix} \begin{pmatrix} 0 \\ 4 \\ 4 \end{pmatrix} \\
&B_3 = \begin{pmatrix} 1 & 3 & 3 \\ 4 & 4 & 4 \end{pmatrix} \begin{pmatrix} 0 \\ 4 \\ 4 \end{pmatrix} \quad \bar{B}_3 = \begin{pmatrix} 3 & 1 & 1 \\ 4 & 4 & 4 \end{pmatrix} \begin{pmatrix} 0 \\ 4 \\ 4 \end{pmatrix} \quad B_4 = \begin{pmatrix} 1 & 1 & 1 \\ 2 & 2 & 4 \end{pmatrix} \begin{pmatrix} 0 \\ 2 \\ 4 \end{pmatrix} \quad \bar{B}_4 = \begin{pmatrix} 1 & 1 & 3 \\ 2 & 2 & 4 \end{pmatrix} \begin{pmatrix} 0 \\ 2 \\ 4 \end{pmatrix} \quad B_5 = \begin{pmatrix} 3 & 1 & 3 \\ 4 & 4 & 4 \end{pmatrix} \begin{pmatrix} 0 \\ 4 \\ 4 \end{pmatrix} \quad \bar{B}_5 = \begin{pmatrix} 1 & 3 & 1 \\ 4 & 4 & 4 \end{pmatrix} \begin{pmatrix} 0 \\ 4 \\ 4 \end{pmatrix} \\
&B_6 = \begin{pmatrix} 1 & 1 & 1 \\ 4 & 2 & 2 \end{pmatrix} \begin{pmatrix} 0 \\ 4 \\ 2 \end{pmatrix} \quad \bar{B}_6 = \begin{pmatrix} 3 & 1 & 1 \\ 4 & 2 & 2 \end{pmatrix} \begin{pmatrix} 0 \\ 4 \\ 2 \end{pmatrix} \quad B_7 = \begin{pmatrix} 1 & 3 \\ 2 & 4 \end{pmatrix} \begin{pmatrix} 0 \\ 4 \end{pmatrix} \quad \bar{B}_7 = \begin{pmatrix} 1 & 1 \\ 2 & 4 \end{pmatrix} \begin{pmatrix} 0 \\ 4 \end{pmatrix} \quad B_8 = \begin{pmatrix} 1 & 0 & 1 \\ 4 & 0 & 2 \end{pmatrix} \begin{pmatrix} 0 \\ 4 \\ 2 \end{pmatrix} \quad \bar{B}_8 = \begin{pmatrix} 3 & 0 & 1 \\ 4 & 0 & 2 \end{pmatrix} \begin{pmatrix} 0 \\ 4 \\ 2 \end{pmatrix} \\
&B_9 = \begin{pmatrix} 1 & 0 & 1 \\ 2 & 0 & 4 \end{pmatrix} \begin{pmatrix} 0 \\ 2 \\ 4 \end{pmatrix} \quad \bar{B}_9 = \begin{pmatrix} 1 & 0 & 3 \\ 2 & 0 & 4 \end{pmatrix} \begin{pmatrix} 0 \\ 2 \\ 4 \end{pmatrix} \quad B_{10} = \begin{pmatrix} 0 & 1 & 1 \\ 0 & 4 & 2 \end{pmatrix} \begin{pmatrix} 0 \\ 4 \\ 2 \end{pmatrix} \quad \bar{B}_{10} = \begin{pmatrix} 0 & 3 & 1 \\ 0 & 4 & 2 \end{pmatrix} \begin{pmatrix} 0 \\ 4 \\ 2 \end{pmatrix} \quad B_{11} = \begin{pmatrix} 0 & 1 & 1 \\ 0 & 2 & 4 \end{pmatrix} \begin{pmatrix} 0 \\ 4 \\ 2 \end{pmatrix} \quad \bar{B}_{11} = \begin{pmatrix} 0 & 1 & 3 \\ 0 & 2 & 4 \end{pmatrix} \begin{pmatrix} 0 \\ 4 \\ 2 \end{pmatrix}
\end{aligned} \tag{2}$$

TABLE S7: Atomic displacement basis for the primary \mathbf{q} points.

	Th _x	Th _y	Th _z	O _x ¹	O _y ¹	O _z ¹	O _x ²	O _y ²	O _z ²
$u_{\Gamma}^{T_{2g}}$	0	0	0	0	0	$\frac{\sqrt{2}}{2}$	0	0	$-\frac{\sqrt{2}}{2}$
	0	0	0	$\frac{\sqrt{2}}{2}$	0	0	$-\frac{\sqrt{2}}{2}$	0	0
	0	0	0	0	$\frac{\sqrt{2}}{2}$	0	0	$-\frac{\sqrt{2}}{2}$	0
$u_{\Gamma}^{T_{1u}}$	$\frac{\sqrt{6}}{3}$	0	0	$-\frac{\sqrt{6}}{6}$	0	0	$-\frac{\sqrt{6}}{6}$	0	0
	0	$\frac{\sqrt{6}}{3}$	0	0	$-\frac{\sqrt{6}}{6}$	0	0	$-\frac{\sqrt{6}}{6}$	0
	0	0	$\frac{\sqrt{6}}{3}$	0	0	$-\frac{\sqrt{6}}{6}$	0	0	$-\frac{\sqrt{6}}{6}$
$u_L^{A_{1g}}$	0	0	0	$\frac{\sqrt{6}}{6}$	$-\frac{\sqrt{6}}{6}$	$-\frac{\sqrt{6}}{6}$	$\frac{\sqrt{6}}{6}$	$-\frac{\sqrt{6}}{6}$	$-\frac{\sqrt{6}}{6}$
$u_L^{E_g}$	0	0	0	$\frac{1}{2}$	$\frac{1}{2}$	0	$\frac{1}{2}$	$\frac{1}{2}$	0
	0	0	0	$-\frac{\sqrt{3}}{6}$	$\frac{\sqrt{3}}{6}$	$-\frac{\sqrt{3}}{3}$	$-\frac{\sqrt{3}}{6}$	$\frac{\sqrt{3}}{6}$	$-\frac{\sqrt{3}}{3}$
$u_L^{A_{2u}}$	$\frac{\sqrt{3}}{3}$	$-\frac{\sqrt{3}}{3}$	$-\frac{\sqrt{3}}{3}$	0	0	0	0	0	0
$u_L^{E_u}$	$\frac{\sqrt{6}}{6}$	$-\frac{\sqrt{6}}{6}$	$\frac{\sqrt{6}}{3}$	0	0	0	0	0	0
	$\frac{\sqrt{2}}{2}$	$\frac{\sqrt{2}}{2}$	0	0	0	0	0	0	0
$u_L^{1A_{2u}}$	0	0	0	$\frac{\sqrt{6}}{6}$	$-\frac{\sqrt{6}}{6}$	$-\frac{\sqrt{6}}{6}$	$-\frac{\sqrt{6}}{6}$	$\frac{\sqrt{6}}{6}$	$\frac{\sqrt{6}}{6}$
$u_L^{1E_u}$	0	0	0	$\frac{\sqrt{3}}{6}$	$-\frac{\sqrt{3}}{6}$	$\frac{\sqrt{3}}{3}$	$-\frac{\sqrt{3}}{6}$	$\frac{\sqrt{3}}{6}$	$-\frac{\sqrt{3}}{3}$
	0	0	0	$\frac{1}{2}$	$\frac{1}{2}$	0	$-\frac{1}{2}$	$-\frac{1}{2}$	0
$u_{L1}^{A_{1g}}$	0	0	0	$-\frac{\sqrt{6}}{6}$	$-\frac{\sqrt{6}}{6}$	$-\frac{\sqrt{6}}{6}$	$-\frac{\sqrt{6}}{6}$	$-\frac{\sqrt{6}}{6}$	$-\frac{\sqrt{6}}{6}$
$u_{L1}^{E_g}$	0	0	0	$-\frac{1}{2}$	$\frac{1}{2}$	0	$-\frac{1}{2}$	$\frac{1}{2}$	0
	0	0	0	$\frac{\sqrt{3}}{6}$	$\frac{\sqrt{3}}{6}$	$-\frac{\sqrt{3}}{3}$	$\frac{\sqrt{3}}{6}$	$\frac{\sqrt{3}}{6}$	$-\frac{\sqrt{3}}{3}$
$u_{L1}^{A_{2u}}$	$\frac{\sqrt{3}}{3}$	$\frac{\sqrt{3}}{3}$	$\frac{\sqrt{3}}{3}$	0	0	0	0	0	0
$u_{L1}^{E_u}$	$\frac{\sqrt{6}}{6}$	$\frac{\sqrt{6}}{6}$	$-\frac{\sqrt{6}}{3}$	0	0	0	0	0	0
	$\frac{\sqrt{2}}{2}$	$-\frac{\sqrt{2}}{2}$	0	0	0	0	0	0	0
$u_{L1}^{1A_{2u}}$	0	0	0	$-\frac{\sqrt{6}}{6}$	$-\frac{\sqrt{6}}{6}$	$-\frac{\sqrt{6}}{6}$	$\frac{\sqrt{6}}{6}$	$\frac{\sqrt{6}}{6}$	$\frac{\sqrt{6}}{6}$
$u_{L1}^{1E_u}$	0	0	0	$-\frac{\sqrt{3}}{6}$	$-\frac{\sqrt{3}}{6}$	$\frac{\sqrt{3}}{3}$	$\frac{\sqrt{3}}{6}$	$\frac{\sqrt{3}}{6}$	$-\frac{\sqrt{3}}{3}$
	0	0	0	$-\frac{1}{2}$	$\frac{1}{2}$	0	$\frac{1}{2}$	$-\frac{1}{2}$	0
$u_{L2}^{A_{1g}}$	0	0	0	$-\frac{\sqrt{6}}{6}$	$\frac{\sqrt{6}}{6}$	$-\frac{\sqrt{6}}{6}$	$-\frac{\sqrt{6}}{6}$	$\frac{\sqrt{6}}{6}$	$-\frac{\sqrt{6}}{6}$
$u_{L2}^{E_g}$	0	0	0	$-\frac{1}{2}$	$-\frac{1}{2}$	0	$-\frac{1}{2}$	$-\frac{1}{2}$	0
	0	0	0	$\frac{\sqrt{3}}{6}$	$-\frac{\sqrt{3}}{6}$	$-\frac{\sqrt{3}}{3}$	$\frac{\sqrt{3}}{6}$	$-\frac{\sqrt{3}}{6}$	$-\frac{\sqrt{3}}{3}$
$u_{L2}^{A_{2u}}$	$-\frac{\sqrt{3}}{3}$	$\frac{\sqrt{3}}{3}$	$-\frac{\sqrt{3}}{3}$	0	0	0	0	0	0
$u_{L2}^{E_u}$	$-\frac{\sqrt{6}}{6}$	$\frac{\sqrt{6}}{6}$	$\frac{\sqrt{6}}{3}$	0	0	0	0	0	0
	$-\frac{\sqrt{2}}{2}$	$-\frac{\sqrt{2}}{2}$	0	0	0	0	0	0	0
$u_{L2}^{1A_{2u}}$	0	0	0	$-\frac{\sqrt{6}}{6}$	$\frac{\sqrt{6}}{6}$	$-\frac{\sqrt{6}}{6}$	$\frac{\sqrt{6}}{6}$	$-\frac{\sqrt{6}}{6}$	$\frac{\sqrt{6}}{6}$
$u_{L2}^{1E_u}$	0	0	0	$-\frac{\sqrt{3}}{6}$	$\frac{\sqrt{3}}{6}$	$\frac{\sqrt{3}}{3}$	$\frac{\sqrt{3}}{6}$	$-\frac{\sqrt{3}}{6}$	$-\frac{\sqrt{3}}{3}$
	0	0	0	$-\frac{1}{2}$	$-\frac{1}{2}$	0	$\frac{1}{2}$	$\frac{1}{2}$	0
$u_{L3}^{A_{1g}}$	0	0	0	$-\frac{\sqrt{6}}{6}$	$-\frac{\sqrt{6}}{6}$	$\frac{\sqrt{6}}{6}$	$-\frac{\sqrt{6}}{6}$	$-\frac{\sqrt{6}}{6}$	$\frac{\sqrt{6}}{6}$
$u_{L3}^{E_g}$	0	0	0	$-\frac{1}{2}$	$\frac{1}{2}$	0	$-\frac{1}{2}$	$\frac{1}{2}$	0
	0	0	0	$\frac{\sqrt{3}}{6}$	$\frac{\sqrt{3}}{6}$	$\frac{\sqrt{3}}{3}$	$\frac{\sqrt{3}}{6}$	$\frac{\sqrt{3}}{6}$	$\frac{\sqrt{3}}{3}$
$u_{L3}^{A_{2u}}$	$-\frac{\sqrt{3}}{3}$	$-\frac{\sqrt{3}}{3}$	$\frac{\sqrt{3}}{3}$	0	0	0	0	0	0
$u_{L3}^{E_u}$	$-\frac{\sqrt{6}}{6}$	$-\frac{\sqrt{6}}{6}$	$-\frac{\sqrt{6}}{3}$	0	0	0	0	0	0
	$-\frac{\sqrt{2}}{2}$	$\frac{\sqrt{2}}{2}$	0	0	0	0	0	0	0

u_{Δ}^E	0	-1	0	0	0	0	0	0	0
u_{Δ}^{1E}	1	0	0	0	0	0	0	0	0
u_{Δ}^{2E}	0	0	0	0	$-\frac{\sqrt{2}}{2}i$	0	0	$\frac{\sqrt{2}}{2}$	0
$u_{\Delta}^{A_1}$	0	0	0	$\frac{\sqrt{2}}{2}i$	0	0	$-\frac{\sqrt{2}}{2}$	0	0
$u_{\Delta}^{1A_1}$	0	0	0	$\frac{\sqrt{2}}{2}i$	0	0	$\frac{\sqrt{2}}{2}$	0	0
$u_{\Delta}^{B_2}$	0	0	0	0	$-\frac{\sqrt{2}}{2}i$	0	0	$-\frac{\sqrt{2}}{2}$	0
$u_{\Delta_1}^E$	1	0	0	0	0	0	0	0	0
$u_{\Delta_1}^{1E}$	0	0	0	$\frac{\sqrt{2}}{2}$	0	0	$-\frac{\sqrt{2}}{2}i$	0	0
$u_{\Delta_1}^{B_2}$	0	0	0	$\frac{\sqrt{2}}{2}$	0	0	$\frac{\sqrt{2}}{2}i$	0	0
$u_{\Delta_1}^E$	0	0	1	0	0	0	0	0	0
$u_{\Delta_1}^{1E}$	0	-1	0	0	0	0	0	0	0
$u_{\Delta_1}^{2E}$	0	0	0	0	0	$\frac{\sqrt{2}}{2}$	0	0	$-\frac{\sqrt{2}}{2}i$
$u_{\Delta_1}^{A_1}$	0	0	0	0	$-\frac{\sqrt{2}}{2}$	0	0	$\frac{\sqrt{2}}{2}i$	0
$u_{\Delta_1}^{1A_1}$	0	0	0	0	$\frac{\sqrt{2}}{2}$	0	0	$\frac{\sqrt{2}}{2}i$	0
$u_{\Delta_1}^{B_2}$	0	0	0	0	0	$-\frac{\sqrt{2}}{2}$	0	0	$-\frac{\sqrt{2}}{2}i$
$u_{\Delta_1}^E$	-1	0	0	0	0	0	0	0	0
$u_{\Delta_1}^{1E}$	0	0	0	$-\frac{\sqrt{2}}{2}i$	0	0	$\frac{\sqrt{2}}{2}$	0	0
$u_{\Delta_1}^{B_2}$	0	0	0	$-\frac{\sqrt{2}}{2}i$	0	0	$-\frac{\sqrt{2}}{2}$	0	0
$u_{\Delta_1}^E$	0	0	-1	0	0	0	0	0	0
$u_{\Delta_1}^{1E}$	0	1	0	0	0	0	0	0	0
$u_{\Delta_1}^{2E}$	0	0	0	0	0	$-\frac{\sqrt{2}}{2}i$	0	0	$\frac{\sqrt{2}}{2}$
$u_{\Delta_1}^{A_1}$	0	0	0	0	$\frac{\sqrt{2}}{2}i$	0	0	$-\frac{\sqrt{2}}{2}$	0
$u_{\Delta_1}^{1A_1}$	0	0	0	0	$\frac{\sqrt{2}}{2}i$	0	0	$\frac{\sqrt{2}}{2}$	0
$u_{\Delta_1}^{B_2}$	0	0	0	0	0	$-\frac{\sqrt{2}}{2}i$	0	0	$-\frac{\sqrt{2}}{2}$
$u_{\Delta_2}^E$	0	0	1	0	0	0	0	0	0
$u_{\Delta_2}^{1E}$	-1	0	0	0	0	0	0	0	0
$u_{\Delta_2}^{2E}$	0	0	0	0	0	$\frac{\sqrt{2}}{2}i$	0	0	$-\frac{\sqrt{2}}{2}$
$u_{\Delta_2}^{A_1}$	0	0	0	0	$-\frac{\sqrt{2}}{2}i$	0	0	$\frac{\sqrt{2}}{2}$	0
$u_{\Delta_2}^{1A_1}$	0	0	0	0	$-\frac{\sqrt{2}}{2}i$	0	0	$-\frac{\sqrt{2}}{2}$	0
$u_{\Delta_2}^{B_2}$	0	0	0	0	0	0	0	0	0
$u_{\Delta_2}^E$	0	0	0	0	0	0	0	0	0
$u_{\Delta_2}^{1E}$	0	0	0	0	0	$\frac{\sqrt{2}}{2}i$	0	0	$-\frac{\sqrt{2}}{2}$
$u_{\Delta_2}^{2E}$	0	0	0	0	$-\frac{\sqrt{2}}{2}i$	0	0	$\frac{\sqrt{2}}{2}$	0
$u_{\Delta_2}^{A_1}$	0	0	0	0	0	$-\frac{\sqrt{2}}{2}$	0	0	$-\frac{\sqrt{2}}{2}i$
$u_{\Delta_2}^{1A_1}$	0	0	0	0	0	$\frac{\sqrt{2}}{2}$	0	0	$\frac{\sqrt{2}}{2}$
$u_{\Delta_2}^{B_2}$	0	0	0	0	0	0	0	0	0
$u_{\Delta_2}^E$	0	0	-1	0	0	0	0	0	0
$u_{\Delta_2}^{1E}$	1	0	0	0	0	0	0	0	0
$u_{\Delta_2}^{2E}$	0	0	0	0	0	$-\frac{\sqrt{2}}{2}$	0	0	$\frac{\sqrt{2}}{2}i$
$u_{\Delta_2}^{A_1}$	0	0	0	0	$\frac{\sqrt{2}}{2}$	0	0	$-\frac{\sqrt{2}}{2}i$	0
$u_{\Delta_2}^{1A_1}$	0	0	0	0	$\frac{\sqrt{2}}{2}$	0	0	$\frac{\sqrt{2}}{2}i$	0
$u_{\Delta_2}^{B_2}$	0	0	0	0	0	0	0	0	0
$u_{\Delta_2}^E$	0	0	0	0	0	0	0	0	0
$u_{\Delta_2}^{1E}$	0	0	0	0	0	$-\frac{\sqrt{2}}{2}i$	0	0	$\frac{\sqrt{2}}{2}i$
$u_{\Delta_2}^{2E}$	0	0	0	0	0	$-\frac{\sqrt{2}}{2}$	0	0	$-\frac{\sqrt{2}}{2}i$
$u_{\Delta_2}^{A_1}$	0	0	0	0	0	$\frac{\sqrt{2}}{2}$	0	0	$\frac{\sqrt{2}}{2}i$

$u_W^{A_1}$	0	0	0	$\frac{1}{2}$	$\frac{1}{2}i$	0	$\frac{1}{2}i$	$\frac{1}{2}$	0
$u_W^{B_1}$	0	0	1	0	0	0	0	0	0
$u_W^{1B_1}$	0	0	0	$\frac{1}{2}$	$-\frac{1}{2}i$	0	$\frac{1}{2}i$	$-\frac{1}{2}$	0
$u_W^{A_2}$	0	0	0	$\frac{1}{2}$	$\frac{1}{2}i$	0	$-\frac{1}{2}i$	$-\frac{1}{2}$	0
$u_W^{B_2}$	0	0	0	$\frac{1}{2}$	$-\frac{1}{2}i$	0	$-\frac{1}{2}i$	$\frac{1}{2}$	0
u_W^E	0	1	0	0	0	0	0	0	0
u_W^{1E}	0	0	0	0	0	$\frac{\sqrt{2}}{2}$	0	0	$-\frac{\sqrt{2}}{2}i$
$u_W^{A_1}$	0	0	0	$\frac{1}{2}i$	$\frac{1}{2}$	0	$\frac{1}{2}$	$\frac{1}{2}i$	0
$u_W^{B_1}$	0	0	-1	0	0	0	0	0	0
$u_W^{1B_1}$	0	0	0	$\frac{1}{2}i$	$-\frac{1}{2}$	0	$\frac{1}{2}$	$-\frac{1}{2}i$	0
$u_W^{A_2}$	0	0	0	$\frac{1}{2}i$	$\frac{1}{2}$	0	$-\frac{1}{2}$	$-\frac{1}{2}i$	0
$u_W^{B_2}$	0	0	0	$\frac{1}{2}i$	$-\frac{1}{2}$	0	$-\frac{1}{2}$	$\frac{1}{2}i$	0
u_W^E	0	-1	0	0	0	0	0	0	0
u_W^{1E}	-1	0	0	0	0	0	0	0	0
$u_W^{A_1}$	0	0	0	0	0	$-\frac{\sqrt{2}}{2}i$	0	0	$\frac{\sqrt{2}}{2}$
$u_W^{B_1}$	0	0	0	0	0	$-\frac{\sqrt{2}}{2}$	0	0	$\frac{\sqrt{2}}{2}i$
$u_{W_1}^{A_1}$	0	0	0	0	$\frac{1}{2}$	$\frac{1}{2}i$	0	$\frac{1}{2}i$	$\frac{1}{2}$
$u_{W_1}^{B_1}$	1	0	0	0	0	0	0	0	0
$u_{W_1}^{1B_1}$	0	0	0	0	$\frac{1}{2}$	$-\frac{1}{2}i$	0	$\frac{1}{2}i$	$-\frac{1}{2}$
$u_{W_1}^{A_2}$	0	0	0	0	$\frac{1}{2}$	$\frac{1}{2}i$	0	$-\frac{1}{2}i$	$-\frac{1}{2}$
$u_{W_1}^{B_2}$	0	0	0	0	$\frac{1}{2}$	$-\frac{1}{2}i$	0	$-\frac{1}{2}i$	$\frac{1}{2}$
$u_{W_1}^E$	0	0	1	0	0	0	0	0	0
$u_{W_1}^{1E}$	0	1	0	0	0	0	0	0	0
$u_{W_1}^{A_1}$	0	0	0	$\frac{\sqrt{2}}{2}$	0	0	$-\frac{\sqrt{2}}{2}i$	0	0
$u_{W_1}^{B_1}$	0	0	0	$\frac{\sqrt{2}}{2}i$	0	0	$-\frac{\sqrt{2}}{2}$	0	0
$u_{W_1}^{1B_1}$	0	0	0	0	$\frac{1}{2}i$	$\frac{1}{2}$	0	$\frac{1}{2}$	$\frac{1}{2}i$
$u_{W_1}^{A_2}$	-1	0	0	0	0	0	0	0	0
$u_{W_1}^{B_2}$	0	0	0	0	$\frac{1}{2}i$	$-\frac{1}{2}$	0	$\frac{1}{2}$	$-\frac{1}{2}i$
$u_{W_1}^E$	0	0	0	0	$\frac{1}{2}i$	$\frac{1}{2}$	0	$-\frac{1}{2}$	$-\frac{1}{2}i$
$u_{W_1}^{1E}$	0	0	0	0	$\frac{1}{2}i$	$-\frac{1}{2}$	0	$-\frac{1}{2}$	$\frac{1}{2}i$
$u_{W_1}^{A_1}$	0	0	-1	0	0	0	0	0	0
$u_{W_1}^{B_1}$	0	-1	0	0	0	0	0	0	0
$u_{W_1}^{1B_1}$	0	0	0	$-\frac{\sqrt{2}}{2}i$	0	0	$\frac{\sqrt{2}}{2}$	0	0
$u_{W_1}^{A_2}$	0	0	0	$-\frac{\sqrt{2}}{2}$	0	0	$\frac{\sqrt{2}}{2}i$	0	0
$u_{W_2}^{A_1}$	0	0	0	$\frac{1}{2}$	0	$\frac{1}{2}i$	$\frac{1}{2}i$	0	$\frac{1}{2}$
$u_{W_2}^{B_1}$	0	-1	0	0	0	0	0	0	0
$u_{W_2}^{1B_1}$	0	0	0	$-\frac{1}{2}$	0	$\frac{1}{2}i$	$-\frac{1}{2}i$	0	$\frac{1}{2}$
$u_{W_2}^{A_2}$	0	0	0	$\frac{1}{2}$	0	$\frac{1}{2}i$	$-\frac{1}{2}i$	0	$-\frac{1}{2}$
$u_{W_2}^{B_2}$	0	0	0	$-\frac{1}{2}$	0	$\frac{1}{2}i$	$\frac{1}{2}i$	0	$-\frac{1}{2}$
$u_{W_2}^E$	0	0	-1	0	0	0	0	0	0

	-1	0	0	0	0	0	0	0	0
1E	0	0	0	0	$-\frac{\sqrt{2}}{2}$	0	0	$\frac{\sqrt{2}}{2}i$	0
u_{W_2}	0	0	0	0	$-\frac{\sqrt{2}}{2}i$	0	0	$\frac{\sqrt{2}}{2}$	0
$u_{W_2}^{A_1}$	0	0	0	$\frac{1}{2}i$	0	$\frac{1}{2}$	$\frac{1}{2}$	0	$\frac{1}{2}i$
$u_{W_2}^{B_1}$	0	1	0	0	0	0	0	0	0
1B_1	0	0	0	$-\frac{1}{2}i$	0	$\frac{1}{2}$	$-\frac{1}{2}$	0	$\frac{1}{2}i$
$u_{W_2}^{A_2}$	0	0	0	$\frac{1}{2}i$	0	$\frac{1}{2}$	$-\frac{1}{2}$	0	$-\frac{1}{2}i$
$u_{W_2}^{B_2}$	0	0	0	$-\frac{1}{2}i$	0	$\frac{1}{2}$	$\frac{1}{2}$	0	$-\frac{1}{2}i$
E	0	0	1	0	0	0	0	0	0
u_{W_2}	1	0	0	0	0	0	0	0	0
1E	0	0	0	0	$\frac{\sqrt{2}}{2}i$	0	0	$-\frac{\sqrt{2}}{2}$	0
u_{W_2}	0	0	0	0	$\frac{\sqrt{2}}{2}$	0	0	$-\frac{\sqrt{2}}{2}i$	0
$u_A^{A_1}$	$\frac{\sqrt{2}}{2}$	$-\frac{\sqrt{2}}{2}$	0	0	0	0	0	0	0
$u_A^{B_2}$	$\frac{\sqrt{2}}{2}$	$\frac{\sqrt{2}}{2}$	0	0	0	0	0	0	0
1A_1	0	0	0	$\frac{1}{2}$	$-\frac{1}{2}$	0	$\frac{1}{2}$	$-\frac{1}{2}$	0
1B_2	0	0	0	$\frac{1}{2}$	$\frac{1}{2}$	0	$\frac{1}{2}$	$\frac{1}{2}$	0
2A_1	0	0	0	0	0	$\frac{\sqrt{2}}{2}$	0	0	$-\frac{\sqrt{2}}{2}$
1B_1	0	0	0	$\frac{1}{2}$	$-\frac{1}{2}$	0	$-\frac{1}{2}$	$\frac{1}{2}$	0
$u_A^{A_2}$	0	0	0	$\frac{1}{2}$	$\frac{1}{2}$	0	$-\frac{1}{2}$	$-\frac{1}{2}$	0
$u_A^{B_1}$	0	0	1	0	0	0	0	0	0
2B_1	0	0	0	0	0	$\frac{\sqrt{2}}{2}$	0	0	$\frac{\sqrt{2}}{2}$
$u_A^{A_1}$	$-\frac{\sqrt{2}}{2}$	$\frac{\sqrt{2}}{2}$	0	0	0	0	0	0	0
$u_A^{B_2}$	$-\frac{\sqrt{2}}{2}$	$-\frac{\sqrt{2}}{2}$	0	0	0	0	0	0	0
1A_1	0	0	0	$-\frac{1}{2}$	$\frac{1}{2}$	0	$-\frac{1}{2}$	$\frac{1}{2}$	0
1B_2	0	0	0	$-\frac{1}{2}$	$-\frac{1}{2}$	0	$-\frac{1}{2}$	$-\frac{1}{2}$	0
2A_1	0	0	0	0	0	$\frac{\sqrt{2}}{2}$	0	0	$-\frac{\sqrt{2}}{2}$
1B_1	0	0	0	$-\frac{1}{2}$	$\frac{1}{2}$	0	$\frac{1}{2}$	$-\frac{1}{2}$	0
$u_A^{A_2}$	0	0	0	$-\frac{1}{2}$	$-\frac{1}{2}$	0	$\frac{1}{2}$	$\frac{1}{2}$	0
$u_A^{B_1}$	0	0	1	0	0	0	0	0	0
2B_1	0	0	0	0	0	$\frac{\sqrt{2}}{2}$	0	0	$\frac{\sqrt{2}}{2}$
$u_{A_1}^{A_1}$	0	$\frac{\sqrt{2}}{2}$	$\frac{\sqrt{2}}{2}$	0	0	0	0	0	0
$u_{A_1}^{B_2}$	0	$\frac{\sqrt{2}}{2}$	$-\frac{\sqrt{2}}{2}$	0	0	0	0	0	0
1A_1	0	0	0	0	$\frac{1}{2}i$	$\frac{1}{2}i$	0	$-\frac{1}{2}i$	$-\frac{1}{2}i$
1B_2	0	0	0	0	$\frac{1}{2}i$	$-\frac{1}{2}i$	0	$-\frac{1}{2}i$	$\frac{1}{2}i$
2A_1	0	0	0	$-\frac{\sqrt{2}}{2}i$	0	0	$-\frac{\sqrt{2}}{2}i$	0	0
1B_1	0	0	0	0	$\frac{1}{2}i$	$\frac{1}{2}i$	0	$\frac{1}{2}i$	$\frac{1}{2}i$
$u_{A_1}^{A_2}$	0	0	0	0	$\frac{1}{2}i$	$-\frac{1}{2}i$	0	$\frac{1}{2}i$	$-\frac{1}{2}i$
$u_{A_1}^{B_1}$	-1	0	0	0	0	0	0	0	0
2B_1	0	0	0	$-\frac{\sqrt{2}}{2}i$	0	0	$\frac{\sqrt{2}}{2}i$	0	0
$u_{A_1}^{A_1}$	0	$-\frac{\sqrt{2}}{2}$	$-\frac{\sqrt{2}}{2}$	0	0	0	0	0	0

$u_{A_1}^{B_2}$	0	$-\frac{\sqrt{2}}{2}$	$\frac{\sqrt{2}}{2}$	0	0	0	0	0	0
$u_{A_1}^{1A_1}$	0	0	0	0	$\frac{1}{2}i$	$\frac{1}{2}i$	0	$-\frac{1}{2}i$	$-\frac{1}{2}i$
$u_{A_1}^{1B_2}$	0	0	0	0	$\frac{1}{2}i$	$-\frac{1}{2}i$	0	$-\frac{1}{2}i$	$\frac{1}{2}i$
$u_{A_1}^{2A_1}$	0	0	0	$\frac{\sqrt{2}}{2}i$	0	0	$\frac{\sqrt{2}}{2}i$	0	0
$u_{A_1}^{1B_1}$	0	0	0	0	$\frac{1}{2}i$	$\frac{1}{2}i$	0	$\frac{1}{2}i$	$\frac{1}{2}i$
$u_{A_1}^{A_2}$	0	0	0	0	$\frac{1}{2}i$	$-\frac{1}{2}i$	0	$\frac{1}{2}i$	$-\frac{1}{2}i$
$u_{A_1}^{B_1}$	-1	0	0	0	0	0	0	0	0
$u_{A_1}^{2B_1}$	0	0	0	$\frac{\sqrt{2}}{2}i$	0	0	$-\frac{\sqrt{2}}{2}i$	0	0
$u_{A_2}^{A_1}$	$\frac{\sqrt{2}}{2}$	0	$-\frac{\sqrt{2}}{2}$	0	0	0	0	0	0
$u_{A_2}^{B_2}$	$-\frac{\sqrt{2}}{2}$	0	$-\frac{\sqrt{2}}{2}$	0	0	0	0	0	0
$u_{A_2}^{1A_1}$	0	0	0	$\frac{1}{2}$	0	$-\frac{1}{2}$	$\frac{1}{2}$	0	$-\frac{1}{2}$
$u_{A_2}^{1B_2}$	0	0	0	$-\frac{1}{2}$	0	$-\frac{1}{2}$	$-\frac{1}{2}$	0	$-\frac{1}{2}$
$u_{A_2}^{2A_1}$	0	0	0	0	$\frac{\sqrt{2}}{2}$	0	0	$-\frac{\sqrt{2}}{2}$	0
$u_{A_2}^{1B_1}$	0	0	0	$\frac{1}{2}$	0	$-\frac{1}{2}$	$-\frac{1}{2}$	0	$\frac{1}{2}$
$u_{A_2}^{A_2}$	0	0	0	$-\frac{1}{2}$	0	$-\frac{1}{2}$	$\frac{1}{2}$	0	$\frac{1}{2}$
$u_{A_2}^{B_1}$	0	1	0	0	0	0	0	0	0
$u_{A_2}^{2B_1}$	0	0	0	0	$\frac{\sqrt{2}}{2}$	0	0	$\frac{\sqrt{2}}{2}$	0
$u_{A_2}^{A_1}$	$-\frac{\sqrt{2}}{2}$	0	$\frac{\sqrt{2}}{2}$	0	0	0	0	0	0
$u_{A_2}^{B_2}$	$\frac{\sqrt{2}}{2}$	0	$\frac{\sqrt{2}}{2}$	0	0	0	0	0	0
$u_{A_2}^{1A_1}$	0	0	0	$-\frac{1}{2}$	0	$\frac{1}{2}$	$-\frac{1}{2}$	0	$\frac{1}{2}$
$u_{A_2}^{1B_2}$	0	0	0	$\frac{1}{2}$	0	$\frac{1}{2}$	$\frac{1}{2}$	0	$\frac{1}{2}$
$u_{A_2}^{2A_1}$	0	0	0	0	$\frac{\sqrt{2}}{2}$	0	0	$-\frac{\sqrt{2}}{2}$	0
$u_{A_2}^{1B_1}$	0	0	0	$-\frac{1}{2}$	0	$\frac{1}{2}$	$\frac{1}{2}$	0	$-\frac{1}{2}$
$u_{A_2}^{A_2}$	0	0	0	$\frac{1}{2}$	0	$\frac{1}{2}$	$-\frac{1}{2}$	0	$-\frac{1}{2}$
$u_{A_2}^{B_1}$	0	1	0	0	0	0	0	0	0
$u_{A_2}^{2B_1}$	0	0	0	0	$\frac{\sqrt{2}}{2}$	0	0	$\frac{\sqrt{2}}{2}$	0
$u_{A_3}^{A_1}$	0	$-\frac{\sqrt{2}}{2}$	$\frac{\sqrt{2}}{2}$	0	0	0	0	0	0
$u_{A_3}^{B_2}$	0	$-\frac{\sqrt{2}}{2}$	$-\frac{\sqrt{2}}{2}$	0	0	0	0	0	0
$u_{A_3}^{1A_1}$	0	0	0	0	$-\frac{1}{2}$	$\frac{1}{2}$	0	$-\frac{1}{2}$	$\frac{1}{2}$
$u_{A_3}^{1B_2}$	0	0	0	0	$-\frac{1}{2}$	$-\frac{1}{2}$	0	$-\frac{1}{2}$	$-\frac{1}{2}$
$u_{A_3}^{2A_1}$	0	0	0	$\frac{\sqrt{2}}{2}$	0	0	$-\frac{\sqrt{2}}{2}$	0	0
$u_{A_3}^{1B_1}$	0	0	0	0	$-\frac{1}{2}$	$\frac{1}{2}$	0	$\frac{1}{2}$	$-\frac{1}{2}$
$u_{A_3}^{A_2}$	0	0	0	0	$-\frac{1}{2}$	$-\frac{1}{2}$	0	$\frac{1}{2}$	$\frac{1}{2}$
$u_{A_3}^{B_1}$	1	0	0	0	0	0	0	0	0
$u_{A_3}^{2B_1}$	0	0	0	$\frac{\sqrt{2}}{2}$	0	0	$\frac{\sqrt{2}}{2}$	0	0
$u_{A_3}^{A_1}$	0	$\frac{\sqrt{2}}{2}$	$-\frac{\sqrt{2}}{2}$	0	0	0	0	0	0
$u_{A_3}^{B_2}$	0	$\frac{\sqrt{2}}{2}$	$\frac{\sqrt{2}}{2}$	0	0	0	0	0	0
$u_{A_3}^{1A_1}$	0	0	0	0	$\frac{1}{2}$	$-\frac{1}{2}$	0	$\frac{1}{2}$	$-\frac{1}{2}$
$u_{A_3}^{1B_2}$	0	0	0	0	$\frac{1}{2}$	$\frac{1}{2}$	0	$\frac{1}{2}$	$\frac{1}{2}$

$u_{A_3}^{2A_1}$	0	0	0	$\frac{\sqrt{2}}{2}$	0	0	$-\frac{\sqrt{2}}{2}$	0	0
$u_{A_3}^{1B_1}$	0	0	0	0	$\frac{1}{2}$	$-\frac{1}{2}$	0	$-\frac{1}{2}$	$\frac{1}{2}$
$u_{A_3}^{A_2}$	0	0	0	0	$\frac{1}{2}$	$\frac{1}{2}$	0	$-\frac{1}{2}$	$-\frac{1}{2}$
$u_{A_3}^{B_1}$	1	0	0	0	0	0	0	0	0
$u_{A_3}^{2B_1}$	0	0	0	$\frac{\sqrt{2}}{2}$	0	0	$\frac{\sqrt{2}}{2}$	0	0
$u_{A_4}^{A_1}$	$\frac{\sqrt{2}}{2}$	0	$\frac{\sqrt{2}}{2}$	0	0	0	0	0	0
$u_{A_4}^{B_2}$	$-\frac{\sqrt{2}}{2}$	0	$\frac{\sqrt{2}}{2}$	0	0	0	0	0	0
$u_{A_4}^{1A_1}$	0	0	0	$\frac{1}{2}i$	0	$\frac{1}{2}i$	$-\frac{1}{2}i$	0	$-\frac{1}{2}i$
$u_{A_4}^{1B_2}$	0	0	0	$-\frac{1}{2}i$	0	$\frac{1}{2}i$	$\frac{1}{2}i$	0	$-\frac{1}{2}i$
$u_{A_4}^{2A_1}$	0	0	0	0	$-\frac{\sqrt{2}}{2}i$	0	0	$-\frac{\sqrt{2}}{2}i$	0
$u_{A_4}^{1B_1}$	0	0	0	$\frac{1}{2}i$	0	$\frac{1}{2}i$	$\frac{1}{2}i$	0	$\frac{1}{2}i$
$u_{A_4}^{A_2}$	0	0	0	$-\frac{1}{2}i$	0	$\frac{1}{2}i$	$-\frac{1}{2}i$	0	$\frac{1}{2}i$
$u_{A_4}^{B_1}$	0	-1	0	0	0	0	0	0	0
$u_{A_4}^{2B_1}$	0	0	0	0	$-\frac{\sqrt{2}}{2}i$	0	0	$\frac{\sqrt{2}}{2}i$	0
$u_{A_4}^{A_1}$	$-\frac{\sqrt{2}}{2}$	0	$-\frac{\sqrt{2}}{2}$	0	0	0	0	0	0
$u_{A_4}^{B_2}$	$\frac{\sqrt{2}}{2}$	0	$-\frac{\sqrt{2}}{2}$	0	0	0	0	0	0
$u_{A_4}^{1A_1}$	0	0	0	$\frac{1}{2}i$	0	$\frac{1}{2}i$	$-\frac{1}{2}i$	0	$-\frac{1}{2}i$
$u_{A_4}^{1B_2}$	0	0	0	$-\frac{1}{2}i$	0	$\frac{1}{2}i$	$\frac{1}{2}i$	0	$-\frac{1}{2}i$
$u_{A_4}^{2A_1}$	0	0	0	0	$\frac{\sqrt{2}}{2}i$	0	0	$\frac{\sqrt{2}}{2}i$	0
$u_{A_4}^{1B_1}$	0	0	0	$\frac{1}{2}i$	0	$\frac{1}{2}i$	$\frac{1}{2}i$	0	$\frac{1}{2}i$
$u_{A_4}^{A_2}$	0	0	0	$-\frac{1}{2}i$	0	$\frac{1}{2}i$	$-\frac{1}{2}i$	0	$\frac{1}{2}i$
$u_{A_4}^{B_1}$	0	-1	0	0	0	0	0	0	0
$u_{A_4}^{2B_1}$	0	0	0	0	$\frac{\sqrt{2}}{2}i$	0	0	$-\frac{\sqrt{2}}{2}i$	0
$u_{A_5}^{A_1}$	$-\frac{\sqrt{2}}{2}$	$-\frac{\sqrt{2}}{2}$	0	0	0	0	0	0	0
$u_{A_5}^{B_2}$	$-\frac{\sqrt{2}}{2}$	$\frac{\sqrt{2}}{2}$	0	0	0	0	0	0	0
$u_{A_5}^{1A_1}$	0	0	0	$\frac{1}{2}i$	$\frac{1}{2}i$	0	$-\frac{1}{2}i$	$-\frac{1}{2}i$	0
$u_{A_5}^{1B_2}$	0	0	0	$\frac{1}{2}i$	$-\frac{1}{2}i$	0	$-\frac{1}{2}i$	$\frac{1}{2}i$	0
$u_{A_5}^{2A_1}$	0	0	0	0	0	$\frac{\sqrt{2}}{2}i$	0	0	$\frac{\sqrt{2}}{2}i$
$u_{A_5}^{1B_1}$	0	0	0	$\frac{1}{2}i$	$\frac{1}{2}i$	0	$\frac{1}{2}i$	$\frac{1}{2}i$	0
$u_{A_5}^{A_2}$	0	0	0	$\frac{1}{2}i$	$-\frac{1}{2}i$	0	$\frac{1}{2}i$	$-\frac{1}{2}i$	0
$u_{A_5}^{B_1}$	0	0	-1	0	0	0	0	0	0
$u_{A_5}^{2B_1}$	0	0	0	0	0	$\frac{\sqrt{2}}{2}i$	0	0	$-\frac{\sqrt{2}}{2}i$
$u_{A_5}^{A_1}$	$\frac{\sqrt{2}}{2}$	$\frac{\sqrt{2}}{2}$	0	0	0	0	0	0	0
$u_{A_5}^{B_2}$	$\frac{\sqrt{2}}{2}$	$-\frac{\sqrt{2}}{2}$	0	0	0	0	0	0	0
$u_{A_5}^{1A_1}$	0	0	0	$\frac{1}{2}i$	$\frac{1}{2}i$	0	$-\frac{1}{2}i$	$-\frac{1}{2}i$	0
$u_{A_5}^{1B_2}$	0	0	0	$\frac{1}{2}i$	$-\frac{1}{2}i$	0	$-\frac{1}{2}i$	$\frac{1}{2}i$	0
$u_{A_5}^{2A_1}$	0	0	0	0	0	$-\frac{\sqrt{2}}{2}i$	0	0	$-\frac{\sqrt{2}}{2}i$
$u_{A_5}^{1B_1}$	0	0	0	$\frac{1}{2}i$	$\frac{1}{2}i$	0	$\frac{1}{2}i$	$\frac{1}{2}i$	0
$u_{A_5}^{A_2}$	0	0	0	$\frac{1}{2}i$	$-\frac{1}{2}i$	0	$\frac{1}{2}i$	$-\frac{1}{2}i$	0

$u_{A_5}^{B_1}$	0	0	-1	0	0	0	0	0	0
$u_{A_5}^{2B_1}$	0	0	0	0	0	$-\frac{\sqrt{2}}{2}i$	0	0	$\frac{\sqrt{2}}{2}i$
$u_{\Lambda}^{A_1}$	$\frac{\sqrt{3}}{3}$	$-\frac{\sqrt{3}}{3}$	$-\frac{\sqrt{3}}{3}$	0	0	0	0	0	0
u_{Λ}^E	$\frac{\sqrt{2}}{2}$	$\frac{\sqrt{2}}{2}$	0	0	0	0	0	0	0
$u_{\Lambda}^{1A_1}$	$-\frac{\sqrt{6}}{6}$	$\frac{\sqrt{6}}{6}$	$-\frac{\sqrt{6}}{3}$	0	0	0	0	0	0
u_{Λ}^{1E}	0	0	0	$\frac{\sqrt{3}}{3}$	$-\frac{\sqrt{3}}{3}$	$-\frac{\sqrt{3}}{3}$	0	0	0
$u_{\Lambda}^{2A_1}$	0	0	0	0	0	0	$\frac{\sqrt{3}}{3}$	$-\frac{\sqrt{3}}{3}$	$-\frac{\sqrt{3}}{3}$
u_{Λ}^{2E}	0	0	0	0	0	0	$\frac{\sqrt{2}}{2}$	$\frac{\sqrt{2}}{2}$	0
$u_{\Lambda}^{A_1}$	$-\frac{\sqrt{3}}{3}$	$\frac{\sqrt{3}}{3}$	$\frac{\sqrt{3}}{3}$	0	0	0	0	0	0
u_{Λ}^E	$-\frac{\sqrt{2}}{2}$	$-\frac{\sqrt{2}}{2}$	0	0	0	0	0	0	0
$u_{\Lambda}^{1A_1}$	0	0	0	0	0	0	$-\frac{\sqrt{3}}{3}i$	$\frac{\sqrt{3}}{3}i$	$\frac{\sqrt{3}}{3}i$
u_{Λ}^{1E}	0	0	0	0	0	0	$-\frac{\sqrt{2}}{2}i$	$-\frac{\sqrt{2}}{2}i$	0
$u_{\Lambda}^{2A_1}$	0	0	0	$-\frac{\sqrt{3}}{3}i$	$\frac{\sqrt{3}}{3}i$	$\frac{\sqrt{3}}{3}i$	0	0	0
u_{Λ}^{2E}	0	0	0	$-\frac{\sqrt{2}}{2}i$	$-\frac{\sqrt{2}}{2}i$	0	0	0	0
$u_{\Lambda_1}^{A_1}$	$\frac{\sqrt{3}}{3}$	$-\frac{\sqrt{3}}{3}$	$\frac{\sqrt{3}}{3}$	0	0	0	0	0	0
$u_{\Lambda_1}^E$	$\frac{\sqrt{2}}{2}$	$\frac{\sqrt{2}}{2}$	0	0	0	0	0	0	0
$u_{\Lambda_1}^{1A_1}$	0	0	0	0	0	0	$\frac{\sqrt{3}}{3}i$	$-\frac{\sqrt{3}}{3}i$	$\frac{\sqrt{3}}{3}i$
$u_{\Lambda_1}^{1E}$	0	0	0	0	0	0	$\frac{\sqrt{2}}{2}i$	$\frac{\sqrt{2}}{2}i$	0
$u_{\Lambda_1}^{2A_1}$	0	0	0	$\frac{\sqrt{3}}{3}i$	$-\frac{\sqrt{3}}{3}i$	$\frac{\sqrt{3}}{3}i$	0	0	0
$u_{\Lambda_1}^{2E}$	0	0	0	$\frac{\sqrt{2}}{2}i$	$\frac{\sqrt{2}}{2}i$	0	0	0	0
$u_{\Lambda_1}^{A_1}$	$-\frac{\sqrt{3}}{3}$	$\frac{\sqrt{3}}{3}$	$-\frac{\sqrt{3}}{3}$	0	0	0	0	0	0
$u_{\Lambda_1}^E$	$-\frac{\sqrt{2}}{2}$	$-\frac{\sqrt{2}}{2}$	0	0	0	0	0	0	0
$u_{\Lambda_1}^{1A_1}$	0	0	0	$-\frac{\sqrt{3}}{3}$	$\frac{\sqrt{3}}{3}$	$-\frac{\sqrt{3}}{3}$	0	0	0
$u_{\Lambda_1}^{1E}$	0	0	0	$-\frac{\sqrt{2}}{2}$	$-\frac{\sqrt{2}}{2}$	0	0	0	0
$u_{\Lambda_1}^{2A_1}$	0	0	0	0	0	0	$-\frac{\sqrt{3}}{3}$	$\frac{\sqrt{3}}{3}$	$-\frac{\sqrt{3}}{3}$
$u_{\Lambda_1}^{2E}$	0	0	0	0	0	0	$-\frac{\sqrt{2}}{2}$	$-\frac{\sqrt{2}}{2}$	0
$u_{\Lambda_2}^{A_1}$	$\frac{\sqrt{3}}{3}$	$\frac{\sqrt{3}}{3}$	$-\frac{\sqrt{3}}{3}$	0	0	0	0	0	0
$u_{\Lambda_2}^E$	$\frac{\sqrt{2}}{2}$	$-\frac{\sqrt{2}}{2}$	0	0	0	0	0	0	0
u_{Λ_2}	$-\frac{\sqrt{6}}{6}$	$-\frac{\sqrt{6}}{6}$	$-\frac{\sqrt{6}}{3}$	0	0	0	0	0	0

$u_{\Lambda_2}^{1A_1}$	0	0	0	0	0	0	$\frac{\sqrt{3}}{3}i$	$\frac{\sqrt{3}}{3}i$	$-\frac{\sqrt{3}}{3}i$
$u_{\Lambda_2}^{1E}$	0	0	0	0	0	0	$\frac{\sqrt{2}}{2}i$	$-\frac{\sqrt{2}}{2}i$	0
$u_{\Lambda_2}^{2A_1}$	0	0	0	$\frac{\sqrt{3}}{3}i$	$\frac{\sqrt{3}}{3}i$	$-\frac{\sqrt{3}}{3}i$	0	0	0
$u_{\Lambda_2}^{2E}$	0	0	0	$\frac{\sqrt{2}}{2}i$	$-\frac{\sqrt{2}}{2}i$	0	0	0	0
$u_{\Lambda_2}^{A_1}$	$-\frac{\sqrt{3}}{3}$	$-\frac{\sqrt{3}}{3}$	$\frac{\sqrt{3}}{3}$	0	0	0	0	0	0
$u_{\Lambda_2}^E$	$-\frac{\sqrt{2}}{2}$	$\frac{\sqrt{2}}{2}$	0	0	0	0	0	0	0
$u_{\Lambda_2}^{1A_1}$	$\frac{\sqrt{6}}{6}$	$\frac{\sqrt{6}}{6}$	$\frac{\sqrt{6}}{3}$	0	0	0	0	0	0
$u_{\Lambda_2}^{1E}$	0	0	0	$-\frac{\sqrt{3}}{3}$	$-\frac{\sqrt{3}}{3}$	$\frac{\sqrt{3}}{3}$	0	0	0
$u_{\Lambda_2}^{2A_1}$	0	0	0	$-\frac{\sqrt{2}}{2}$	$\frac{\sqrt{2}}{2}$	0	0	0	0
$u_{\Lambda_2}^{2E}$	0	0	0	$\frac{\sqrt{6}}{6}$	$\frac{\sqrt{6}}{6}$	$\frac{\sqrt{6}}{3}$	0	0	0
$u_{\Lambda_2}^{A_1}$	0	0	0	0	0	0	$-\frac{\sqrt{3}}{3}$	$-\frac{\sqrt{3}}{3}$	$\frac{\sqrt{3}}{3}$
$u_{\Lambda_2}^E$	0	0	0	0	0	0	$-\frac{\sqrt{2}}{2}$	$\frac{\sqrt{2}}{2}$	0
$u_{\Lambda_3}^{1A_1}$	0	0	0	0	0	0	$\frac{\sqrt{6}}{6}$	$\frac{\sqrt{6}}{6}$	$\frac{\sqrt{6}}{3}$
$u_{\Lambda_3}^{1E}$	$-\frac{\sqrt{3}}{3}$	$-\frac{\sqrt{3}}{3}$	$-\frac{\sqrt{3}}{3}$	0	0	0	0	0	0
$u_{\Lambda_3}^{2A_1}$	$-\frac{\sqrt{2}}{2}$	$\frac{\sqrt{2}}{2}$	0	0	0	0	0	0	0
$u_{\Lambda_3}^{2E}$	$\frac{\sqrt{6}}{6}$	$\frac{\sqrt{6}}{6}$	$-\frac{\sqrt{6}}{3}$	0	0	0	0	0	0
$u_{\Lambda_3}^{A_1}$	0	0	0	0	0	0	$\frac{\sqrt{3}}{3}$	$\frac{\sqrt{3}}{3}$	$\frac{\sqrt{3}}{3}$
$u_{\Lambda_3}^E$	0	0	0	0	0	0	$\frac{\sqrt{2}}{2}$	$-\frac{\sqrt{2}}{2}$	0
$u_{\Lambda_3}^{1A_1}$	0	0	0	0	0	0	$-\frac{\sqrt{6}}{6}$	$-\frac{\sqrt{6}}{6}$	$\frac{\sqrt{6}}{3}$
$u_{\Lambda_3}^{1E}$	0	0	0	$-\frac{\sqrt{3}}{3}$	$-\frac{\sqrt{3}}{3}$	$-\frac{\sqrt{3}}{3}$	0	0	0
$u_{\Lambda_3}^{2A_1}$	0	0	0	$-\frac{\sqrt{2}}{2}$	$\frac{\sqrt{2}}{2}$	0	0	0	0
$u_{\Lambda_3}^{2E}$	0	0	0	$\frac{\sqrt{6}}{6}$	$\frac{\sqrt{6}}{6}$	$-\frac{\sqrt{6}}{3}$	0	0	0
$u_{\Lambda_3}^{A_1}$	$\frac{\sqrt{3}}{3}$	$\frac{\sqrt{3}}{3}$	$\frac{\sqrt{3}}{3}$	0	0	0	0	0	0
$u_{\Lambda_3}^E$	$\frac{\sqrt{2}}{2}$	$-\frac{\sqrt{2}}{2}$	0	0	0	0	0	0	0
$u_{\Lambda_3}^{1A_1}$	$-\frac{\sqrt{6}}{6}$	$-\frac{\sqrt{6}}{6}$	$\frac{\sqrt{6}}{3}$	0	0	0	0	0	0
$u_{\Lambda_3}^{1E}$	0	0	0	$\frac{\sqrt{3}}{3}i$	$\frac{\sqrt{3}}{3}i$	$\frac{\sqrt{3}}{3}i$	0	0	0
$u_{\Lambda_3}^{2A_1}$	0	0	0	$\frac{\sqrt{2}}{2}i$	$-\frac{\sqrt{2}}{2}i$	0	0	0	0
$u_{\Lambda_3}^{2E}$	0	0	0	$-\frac{\sqrt{6}}{6}i$	$-\frac{\sqrt{6}}{6}i$	$\frac{\sqrt{6}}{3}i$	0	0	0
$u_{\Lambda_3}^{A_1}$	0	0	0	0	0	0	$-\frac{\sqrt{3}}{3}i$	$-\frac{\sqrt{3}}{3}i$	$-\frac{\sqrt{3}}{3}i$
$u_{\Lambda_3}^E$	0	0	0	0	0	0	$-\frac{\sqrt{2}}{2}i$	$\frac{\sqrt{2}}{2}i$	0
u_B^A	$\frac{\sqrt{2}}{2}$	$-\frac{\sqrt{2}}{2}$	0	0	0	0	0	0	0
u_B^B	$\frac{\sqrt{2}}{2}$	$\frac{\sqrt{2}}{2}$	0	0	0	0	0	0	0
u_B^{1A}	0	0	1	0	0	0	0	0	0
u_B^{2A}	0	0	0	$\frac{\sqrt{2}}{2}$	$-\frac{\sqrt{2}}{2}$	0	0	0	0
u_B^{1B}	0	0	0	$\frac{\sqrt{2}}{2}$	$\frac{\sqrt{2}}{2}$	0	0	0	0
u_B^{3A}	0	0	0	0	0	1	0	0	0
u_B^{4A}	0	0	0	0	0	0	$\frac{\sqrt{2}}{2}$	$-\frac{\sqrt{2}}{2}$	0

u_B^{2B}	0	0	0	0	0	0	$\frac{\sqrt{2}}{2}$	$\frac{\sqrt{2}}{2}$	0
u_B^{5A}	0	0	0	0	0	0	0	0	1
$u_{\bar{B}}^A$	$-\frac{\sqrt{2}}{2}$	$\frac{\sqrt{2}}{2}$	0	0	0	0	0	0	0
$u_{\bar{B}}^B$	$-\frac{\sqrt{2}}{2}$	$-\frac{\sqrt{2}}{2}$	0	0	0	0	0	0	0
$u_{\bar{B}}^{1A}$	0	0	-1	0	0	0	0	0	0
$u_{\bar{B}}^{2A}$	0	0	0	0	0	0	$\frac{\sqrt{2}}{2}i$	$-\frac{\sqrt{2}}{2}i$	0
$u_{\bar{B}}^{1B}$	0	0	0	0	0	0	$\frac{\sqrt{2}}{2}i$	$\frac{\sqrt{2}}{2}i$	0
$u_{\bar{B}}^{3A}$	0	0	0	0	0	0	0	0	$1i$
$u_{\bar{B}}^{4A}$	0	0	0	$\frac{\sqrt{2}}{2}i$	$-\frac{\sqrt{2}}{2}i$	0	0	0	0
$u_{\bar{B}}^{2B}$	0	0	0	$\frac{\sqrt{2}}{2}i$	$\frac{\sqrt{2}}{2}i$	0	0	0	0
$u_{\bar{B}}^{5A}$	0	0	0	0	0	$1i$	0	0	0
$u_{B_1}^A$	$-\frac{\sqrt{2}}{2}$	0	$-\frac{\sqrt{2}}{2}$	0	0	0	0	0	0
$u_{B_1}^B$	$\frac{\sqrt{2}}{2}$	0	$-\frac{\sqrt{2}}{2}$	0	0	0	0	0	0
$u_{B_1}^{1A}$	0	-1	0	0	0	0	0	0	0
$u_{B_1}^{2A}$	0	0	0	$\frac{\sqrt{2}}{2}$	0	$\frac{\sqrt{2}}{2}$	0	0	0
$u_{B_1}^{1B}$	0	0	0	$-\frac{\sqrt{2}}{2}$	0	$\frac{\sqrt{2}}{2}$	0	0	0
$u_{B_1}^{3A}$	0	0	0	0	1	0	0	0	0
$u_{B_1}^{4A}$	0	0	0	0	0	0	$\frac{\sqrt{2}}{2}$	0	$\frac{\sqrt{2}}{2}$
$u_{B_1}^{2B}$	0	0	0	0	0	0	$-\frac{\sqrt{2}}{2}$	0	$\frac{\sqrt{2}}{2}$
$u_{B_1}^{5A}$	0	0	0	0	0	0	0	1	0
$u_{\bar{B}_1}^A$	$\frac{\sqrt{2}}{2}$	0	$\frac{\sqrt{2}}{2}$	0	0	0	0	0	0
$u_{\bar{B}_1}^B$	$-\frac{\sqrt{2}}{2}$	0	$\frac{\sqrt{2}}{2}$	0	0	0	0	0	0
$u_{\bar{B}_1}^{1A}$	0	1	0	0	0	0	0	0	0
$u_{\bar{B}_1}^{2A}$	0	0	0	0	0	0	$\frac{\sqrt{2}}{2}i$	0	$\frac{\sqrt{2}}{2}i$
$u_{\bar{B}_1}^{1B}$	0	0	0	0	0	0	$-\frac{\sqrt{2}}{2}i$	0	$\frac{\sqrt{2}}{2}i$
$u_{\bar{B}_1}^{3A}$	0	0	0	0	0	0	0	$1i$	0
$u_{\bar{B}_1}^{4A}$	0	0	0	$\frac{\sqrt{2}}{2}i$	0	$\frac{\sqrt{2}}{2}i$	0	0	0
$u_{\bar{B}_1}^{2B}$	0	0	0	$-\frac{\sqrt{2}}{2}i$	0	$\frac{\sqrt{2}}{2}i$	0	0	0
$u_{\bar{B}_1}^{5A}$	0	0	0	0	$1i$	0	0	0	0
$u_{B_2}^A$	$\frac{\sqrt{2}}{2}$	$\frac{\sqrt{2}}{2}$	0	0	0	0	0	0	0
$u_{B_2}^B$	$\frac{\sqrt{2}}{2}$	$-\frac{\sqrt{2}}{2}$	0	0	0	0	0	0	0
$u_{B_2}^{1A}$	0	0	-1	0	0	0	0	0	0
$u_{B_2}^{2A}$	0	0	0	$\frac{\sqrt{2}}{2}i$	$\frac{\sqrt{2}}{2}i$	0	0	0	0
$u_{B_2}^{1B}$	0	0	0	$\frac{\sqrt{2}}{2}i$	$-\frac{\sqrt{2}}{2}i$	0	0	0	0
$u_{B_2}^{3A}$	0	0	0	0	0	$-1i$	0	0	0
$u_{B_2}^{4A}$	0	0	0	0	0	0	$-\frac{\sqrt{2}}{2}i$	$-\frac{\sqrt{2}}{2}i$	0
$u_{B_2}^{2B}$	0	0	0	0	0	0	$-\frac{\sqrt{2}}{2}i$	$\frac{\sqrt{2}}{2}i$	0
$u_{B_2}^{5A}$	0	0	0	0	0	0	0	0	$1i$
$u_{\bar{B}_2}^A$	$-\frac{\sqrt{2}}{2}$	$-\frac{\sqrt{2}}{2}$	0	0	0	0	0	0	0

$u_{\bar{B}_2}^B$	$-\frac{\sqrt{2}}{2}$	$\frac{\sqrt{2}}{2}$	0	0	0	0	0	0	0
$u_{\bar{B}_2}^{1A}$	0	0	1	0	0	0	0	0	0
$u_{\bar{B}_2}^{2A}$	0	0	0	0	0	0	$-\frac{\sqrt{2}}{2}$	$-\frac{\sqrt{2}}{2}$	0
$u_{\bar{B}_2}^{1B}$	0	0	0	0	0	0	$-\frac{\sqrt{2}}{2}$	$\frac{\sqrt{2}}{2}$	0
$u_{\bar{B}_2}^{3A}$	0	0	0	0	0	0	0	0	1
$u_{\bar{B}_2}^{4A}$	0	0	0	$\frac{\sqrt{2}}{2}$	$\frac{\sqrt{2}}{2}$	0	0	0	0
$u_{\bar{B}_2}^{2B}$	0	0	0	$\frac{\sqrt{2}}{2}$	$-\frac{\sqrt{2}}{2}$	0	0	0	0
$u_{\bar{B}_2}^{5A}$	0	0	0	0	0	-1	0	0	0
$u_{B_3}^A$	0	$\frac{\sqrt{2}}{2}$	$\frac{\sqrt{2}}{2}$	0	0	0	0	0	0
$u_{B_3}^B$	0	$\frac{\sqrt{2}}{2}$	$-\frac{\sqrt{2}}{2}$	0	0	0	0	0	0
$u_{B_3}^{1A}$	-1	0	0	0	0	0	0	0	0
$u_{B_3}^{2A}$	0	0	0	0	$\frac{\sqrt{2}}{2}i$	$\frac{\sqrt{2}}{2}i$	0	0	0
$u_{B_3}^{1B}$	0	0	0	0	$\frac{\sqrt{2}}{2}i$	$-\frac{\sqrt{2}}{2}i$	0	0	0
$u_{B_3}^{3A}$	0	0	0	-1i	0	0	0	0	0
$u_{B_3}^{4A}$	0	0	0	0	0	0	0	$-\frac{\sqrt{2}}{2}i$	$-\frac{\sqrt{2}}{2}i$
$u_{B_3}^{2B}$	0	0	0	0	0	0	0	$-\frac{\sqrt{2}}{2}i$	$\frac{\sqrt{2}}{2}i$
$u_{B_3}^{5A}$	0	0	0	0	0	0	1i	0	0
$u_{\bar{B}_3}^A$	0	$-\frac{\sqrt{2}}{2}$	$-\frac{\sqrt{2}}{2}$	0	0	0	0	0	0
$u_{\bar{B}_3}^B$	0	$-\frac{\sqrt{2}}{2}$	$\frac{\sqrt{2}}{2}$	0	0	0	0	0	0
$u_{\bar{B}_3}^{1A}$	1	0	0	0	0	0	0	0	0
$u_{\bar{B}_3}^{2A}$	0	0	0	0	0	0	0	$-\frac{\sqrt{2}}{2}$	$-\frac{\sqrt{2}}{2}$
$u_{\bar{B}_3}^{1B}$	0	0	0	0	0	0	0	$-\frac{\sqrt{2}}{2}$	$\frac{\sqrt{2}}{2}$
$u_{\bar{B}_3}^{3A}$	0	0	0	0	0	0	1	0	0
$u_{\bar{B}_3}^{4A}$	0	0	0	0	$\frac{\sqrt{2}}{2}$	$\frac{\sqrt{2}}{2}$	0	0	0
$u_{\bar{B}_3}^{2B}$	0	0	0	0	$\frac{\sqrt{2}}{2}$	$-\frac{\sqrt{2}}{2}$	0	0	0
$u_{\bar{B}_3}^{5A}$	0	0	0	-1	0	0	0	0	0
$u_{B_4}^A$	$\frac{\sqrt{2}}{2}$	$\frac{\sqrt{2}}{2}$	0	0	0	0	0	0	0
$u_{B_4}^B$	$\frac{\sqrt{2}}{2}$	$-\frac{\sqrt{2}}{2}$	0	0	0	0	0	0	0
$u_{B_4}^{1A}$	0	0	1	0	0	0	0	0	0
$u_{B_4}^{2A}$	0	0	0	0	0	0	$\frac{\sqrt{2}}{2}i$	$\frac{\sqrt{2}}{2}i$	0
$u_{B_4}^{1B}$	0	0	0	0	0	0	$\frac{\sqrt{2}}{2}i$	$-\frac{\sqrt{2}}{2}i$	0
$u_{B_4}^{3A}$	0	0	0	0	0	0	0	0	1i
$u_{B_4}^{4A}$	0	0	0	$\frac{\sqrt{2}}{2}i$	$\frac{\sqrt{2}}{2}i$	0	0	0	0
$u_{B_4}^{2B}$	0	0	0	$\frac{\sqrt{2}}{2}i$	$-\frac{\sqrt{2}}{2}i$	0	0	0	0
$u_{B_4}^{5A}$	0	0	0	0	0	1i	0	0	0
$u_{\bar{B}_4}^A$	$-\frac{\sqrt{2}}{2}$	$-\frac{\sqrt{2}}{2}$	0	0	0	0	0	0	0
$u_{\bar{B}_4}^B$	$-\frac{\sqrt{2}}{2}$	$\frac{\sqrt{2}}{2}$	0	0	0	0	0	0	0
$u_{\bar{B}_4}^{1A}$	0	0	-1	0	0	0	0	0	0

$u_{\bar{B}_4}^{2A}$	0	0	0	$\frac{\sqrt{2}}{2}$	$\frac{\sqrt{2}}{2}$	0	0	0	0
$u_{\bar{B}_4}^{1B}$	0	0	0	$\frac{\sqrt{2}}{2}$	$-\frac{\sqrt{2}}{2}$	0	0	0	0
$u_{\bar{B}_4}^{3A}$	0	0	0	0	0	1	0	0	0
$u_{\bar{B}_4}^{4A}$	0	0	0	0	0	0	$\frac{\sqrt{2}}{2}$	$\frac{\sqrt{2}}{2}$	0
$u_{\bar{B}_4}^{2B}$	0	0	0	0	0	0	$\frac{\sqrt{2}}{2}$	$-\frac{\sqrt{2}}{2}$	0
$u_{\bar{B}_4}^{5A}$	0	0	0	0	0	0	0	0	1
$u_{B_5}^A$	$\frac{\sqrt{2}}{2}$	0	$\frac{\sqrt{2}}{2}$	0	0	0	0	0	0
$u_{B_5}^B$	$-\frac{\sqrt{2}}{2}$	0	$\frac{\sqrt{2}}{2}$	0	0	0	0	0	0
$u_{B_5}^{1A}$	0	-1	0	0	0	0	0	0	0
$u_{B_5}^{2A}$	0	0	0	$\frac{\sqrt{2}}{2}i$	0	$\frac{\sqrt{2}}{2}i$	0	0	0
$u_{B_5}^{1B}$	0	0	0	$-\frac{\sqrt{2}}{2}i$	0	$\frac{\sqrt{2}}{2}i$	0	0	0
$u_{B_5}^{3A}$	0	0	0	0	-1i	0	0	0	0
$u_{B_5}^{4A}$	0	0	0	0	0	0	$-\frac{\sqrt{2}}{2}i$	0	$-\frac{\sqrt{2}}{2}i$
$u_{B_5}^{2B}$	0	0	0	0	0	0	$\frac{\sqrt{2}}{2}i$	0	$-\frac{\sqrt{2}}{2}i$
$u_{B_5}^{5A}$	0	0	0	0	0	0	0	1i	0
$u_{\bar{B}_5}^A$	$-\frac{\sqrt{2}}{2}$	0	$-\frac{\sqrt{2}}{2}$	0	0	0	0	0	0
$u_{\bar{B}_5}^B$	$\frac{\sqrt{2}}{2}$	0	$-\frac{\sqrt{2}}{2}$	0	0	0	0	0	0
$u_{\bar{B}_5}^{1A}$	0	1	0	0	0	0	0	0	0
$u_{\bar{B}_5}^{2A}$	0	0	0	0	0	0	$-\frac{\sqrt{2}}{2}$	0	$-\frac{\sqrt{2}}{2}$
$u_{\bar{B}_5}^{1B}$	0	0	0	0	0	0	$\frac{\sqrt{2}}{2}$	0	$-\frac{\sqrt{2}}{2}$
$u_{\bar{B}_5}^{3A}$	0	0	0	0	0	0	0	1	0
$u_{\bar{B}_5}^{4A}$	0	0	0	$\frac{\sqrt{2}}{2}$	0	$\frac{\sqrt{2}}{2}$	0	0	0
$u_{\bar{B}_5}^{2B}$	0	0	0	$-\frac{\sqrt{2}}{2}$	0	$\frac{\sqrt{2}}{2}$	0	0	0
$u_{\bar{B}_5}^{5A}$	0	0	0	0	-1	0	0	0	0
$u_{B_6}^A$	0	$\frac{\sqrt{2}}{2}$	$\frac{\sqrt{2}}{2}$	0	0	0	0	0	0
$u_{B_6}^B$	0	$\frac{\sqrt{2}}{2}$	$-\frac{\sqrt{2}}{2}$	0	0	0	0	0	0
$u_{B_6}^{1A}$	1	0	0	0	0	0	0	0	0
$u_{B_6}^{2A}$	0	0	0	0	0	0	0	$\frac{\sqrt{2}}{2}i$	$\frac{\sqrt{2}}{2}i$
$u_{B_6}^{1B}$	0	0	0	0	0	0	0	$\frac{\sqrt{2}}{2}i$	$-\frac{\sqrt{2}}{2}i$
$u_{B_6}^{3A}$	0	0	0	0	0	0	1i	0	0
$u_{B_6}^{4A}$	0	0	0	0	$\frac{\sqrt{2}}{2}i$	$\frac{\sqrt{2}}{2}i$	0	0	0
$u_{B_6}^{2B}$	0	0	0	0	$\frac{\sqrt{2}}{2}i$	$-\frac{\sqrt{2}}{2}i$	0	0	0
$u_{B_6}^{5A}$	0	0	0	1i	0	0	0	0	0
$u_{\bar{B}_6}^A$	0	$-\frac{\sqrt{2}}{2}$	$-\frac{\sqrt{2}}{2}$	0	0	0	0	0	0
$u_{\bar{B}_6}^B$	0	$-\frac{\sqrt{2}}{2}$	$\frac{\sqrt{2}}{2}$	0	0	0	0	0	0
$u_{\bar{B}_6}^{1A}$	-1	0	0	0	0	0	0	0	0
$u_{\bar{B}_6}^{2A}$	0	0	0	0	$\frac{\sqrt{2}}{2}$	$\frac{\sqrt{2}}{2}$	0	0	0
$u_{\bar{B}_6}^{1B}$	0	0	0	0	$\frac{\sqrt{2}}{2}$	$-\frac{\sqrt{2}}{2}$	0	0	0

$u_{\bar{B}_6}^{3A}$	0	0	0	1	0	0	0	0	0
$u_{\bar{B}_6}^{4A}$	0	0	0	0	0	0	0	$\frac{\sqrt{2}}{2}$	$\frac{\sqrt{2}}{2}$
$u_{\bar{B}_6}^{2B}$	0	0	0	0	0	0	0	$\frac{\sqrt{2}}{2}$	$-\frac{\sqrt{2}}{2}$
$u_{\bar{B}_6}^{5A}$	0	0	0	0	0	0	1	0	0
$u_{B_7}^A$	$\frac{\sqrt{2}}{2}$	$-\frac{\sqrt{2}}{2}$	0	0	0	0	0	0	0
$u_{B_7}^B$	$\frac{\sqrt{2}}{2}$	$\frac{\sqrt{2}}{2}$	0	0	0	0	0	0	0
$u_{B_7}^{1A}$	0	0	-1	0	0	0	0	0	0
$u_{B_7}^{2A}$	0	0	0	0	0	$-\frac{\sqrt{2}}{2}i$	$\frac{\sqrt{2}}{2}i$	0	0
$u_{B_7}^{1B}$	0	0	0	0	0	$-\frac{\sqrt{2}}{2}i$	$-\frac{\sqrt{2}}{2}i$	0	0
$u_{B_7}^{3A}$	0	0	0	0	0	0	0	0	$1i$
$u_{B_7}^{4A}$	0	0	0	$-\frac{\sqrt{2}}{2}i$	$\frac{\sqrt{2}}{2}i$	0	0	0	0
$u_{B_7}^{2B}$	0	0	0	$-\frac{\sqrt{2}}{2}i$	$-\frac{\sqrt{2}}{2}i$	0	0	0	0
$u_{B_7}^{5A}$	0	0	0	0	0	$1i$	0	0	0
$u_{\bar{B}_7}^A$	$-\frac{\sqrt{2}}{2}$	$\frac{\sqrt{2}}{2}$	0	0	0	0	0	0	0
$u_{\bar{B}_7}^B$	$-\frac{\sqrt{2}}{2}$	$-\frac{\sqrt{2}}{2}$	0	0	0	0	0	0	0
$u_{\bar{B}_7}^{1A}$	0	0	1	0	0	0	0	0	0
$u_{\bar{B}_7}^{2A}$	0	0	0	$-\frac{\sqrt{2}}{2}$	$\frac{\sqrt{2}}{2}$	0	0	0	0
$u_{\bar{B}_7}^{1B}$	0	0	0	$-\frac{\sqrt{2}}{2}$	$-\frac{\sqrt{2}}{2}$	0	0	0	0
$u_{\bar{B}_7}^{3A}$	0	0	0	0	0	1	0	0	0
$u_{\bar{B}_7}^{4A}$	0	0	0	0	0	0	$-\frac{\sqrt{2}}{2}$	$\frac{\sqrt{2}}{2}$	0
$u_{\bar{B}_7}^{2B}$	0	0	0	0	0	0	$-\frac{\sqrt{2}}{2}$	$-\frac{\sqrt{2}}{2}$	0
$u_{\bar{B}_7}^{5A}$	0	0	0	0	0	0	0	0	1
$u_{B_8}^A$	$\frac{\sqrt{2}}{2}$	0	$-\frac{\sqrt{2}}{2}$	0	0	0	0	0	0
$u_{B_8}^B$	$-\frac{\sqrt{2}}{2}$	0	$-\frac{\sqrt{2}}{2}$	0	0	0	0	0	0
$u_{B_8}^{1A}$	0	1	0	0	0	0	0	0	0
$u_{B_8}^{2A}$	0	0	0	$\frac{\sqrt{2}}{2}$	0	$-\frac{\sqrt{2}}{2}$	0	0	0
$u_{B_8}^{1B}$	0	0	0	$-\frac{\sqrt{2}}{2}$	0	$-\frac{\sqrt{2}}{2}$	0	0	0
$u_{B_8}^{3A}$	0	0	0	0	1	0	0	0	0
$u_{B_8}^{4A}$	0	0	0	0	0	0	$\frac{\sqrt{2}}{2}$	0	$-\frac{\sqrt{2}}{2}$
$u_{B_8}^{2B}$	0	0	0	0	0	0	$-\frac{\sqrt{2}}{2}$	0	$-\frac{\sqrt{2}}{2}$
$u_{B_8}^{5A}$	0	0	0	0	0	0	0	1	0
$u_{\bar{B}_8}^A$	$-\frac{\sqrt{2}}{2}$	0	$\frac{\sqrt{2}}{2}$	0	0	0	0	0	0
$u_{\bar{B}_8}^B$	$\frac{\sqrt{2}}{2}$	0	$\frac{\sqrt{2}}{2}$	0	0	0	0	0	0
$u_{\bar{B}_8}^{1A}$	0	-1	0	0	0	0	0	0	0
$u_{\bar{B}_8}^{2A}$	0	0	0	0	0	0	$\frac{\sqrt{2}}{2}i$	0	$-\frac{\sqrt{2}}{2}i$
$u_{\bar{B}_8}^{1B}$	0	0	0	0	0	0	$-\frac{\sqrt{2}}{2}i$	0	$-\frac{\sqrt{2}}{2}i$
$u_{\bar{B}_8}^{3A}$	0	0	0	0	0	0	0	$1i$	0
$u_{\bar{B}_8}^{4A}$	0	0	0	$\frac{\sqrt{2}}{2}i$	0	$-\frac{\sqrt{2}}{2}i$	0	0	0

$u_{B_8}^{2B}$	0	0	0	$-\frac{\sqrt{2}}{2}i$	0	$-\frac{\sqrt{2}}{2}i$	0	0	0
$u_{B_8}^{5A}$	0	0	0	0	$1i$	0	0	0	0
$u_{B_9}^A$	$-\frac{\sqrt{2}}{2}$	0	$\frac{\sqrt{2}}{2}$	0	0	0	0	0	0
$u_{B_9}^B$	$\frac{\sqrt{2}}{2}$	0	$\frac{\sqrt{2}}{2}$	0	0	0	0	0	0
$u_{B_9}^{1A}$	0	1	0	0	0	0	0	0	0
$u_{B_9}^{2A}$	0	0	0	$-\frac{\sqrt{2}}{2}$	0	$\frac{\sqrt{2}}{2}$	0	0	0
$u_{B_9}^{1B}$	0	0	0	$\frac{\sqrt{2}}{2}$	0	$\frac{\sqrt{2}}{2}$	0	0	0
$u_{B_9}^{3A}$	0	0	0	0	1	0	0	0	0
$u_{B_9}^{4A}$	0	0	0	0	0	0	$-\frac{\sqrt{2}}{2}$	0	$\frac{\sqrt{2}}{2}$
$u_{B_9}^{2B}$	0	0	0	0	0	0	$\frac{\sqrt{2}}{2}$	0	$\frac{\sqrt{2}}{2}$
$u_{B_9}^{5A}$	0	0	0	0	0	0	0	1	0
$u_{B_9}^A$	$\frac{\sqrt{2}}{2}$	0	$-\frac{\sqrt{2}}{2}$	0	0	0	0	0	0
$u_{B_9}^B$	$-\frac{\sqrt{2}}{2}$	0	$-\frac{\sqrt{2}}{2}$	0	0	0	0	0	0
$u_{B_9}^{1A}$	0	-1	0	0	0	0	0	0	0
$u_{B_9}^{2A}$	0	0	0	0	0	0	$-\frac{\sqrt{2}}{2}i$	0	$\frac{\sqrt{2}}{2}i$
$u_{B_9}^{1B}$	0	0	0	0	0	0	$\frac{\sqrt{2}}{2}i$	0	$\frac{\sqrt{2}}{2}i$
$u_{B_9}^{3A}$	0	0	0	0	0	0	0	$1i$	0
$u_{B_9}^{4A}$	0	0	0	$-\frac{\sqrt{2}}{2}i$	0	$\frac{\sqrt{2}}{2}i$	0	0	0
$u_{B_9}^{2B}$	0	0	0	$\frac{\sqrt{2}}{2}i$	0	$\frac{\sqrt{2}}{2}i$	0	0	0
$u_{B_9}^{5A}$	0	0	0	0	$1i$	0	0	0	0
$u_{B_{10}}^A$	0	$\frac{\sqrt{2}}{2}$	$-\frac{\sqrt{2}}{2}$	0	0	0	0	0	0
$u_{B_{10}}^B$	0	$\frac{\sqrt{2}}{2}$	$\frac{\sqrt{2}}{2}$	0	0	0	0	0	0
$u_{B_{10}}^{1A}$	1	0	0	0	0	0	0	0	0
$u_{B_{10}}^{2A}$	0	0	0	0	$\frac{\sqrt{2}}{2}$	$-\frac{\sqrt{2}}{2}$	0	0	0
$u_{B_{10}}^{1B}$	0	0	0	0	$\frac{\sqrt{2}}{2}$	$\frac{\sqrt{2}}{2}$	0	0	0
$u_{B_{10}}^{3A}$	0	0	0	1	0	0	0	0	0
$u_{B_{10}}^{4A}$	0	0	0	0	0	0	0	$\frac{\sqrt{2}}{2}$	$-\frac{\sqrt{2}}{2}$
$u_{B_{10}}^{2B}$	0	0	0	0	0	0	0	$\frac{\sqrt{2}}{2}$	$\frac{\sqrt{2}}{2}$
$u_{B_{10}}^{5A}$	0	0	0	0	0	0	1	0	0
$u_{B_{10}}^A$	0	$-\frac{\sqrt{2}}{2}$	$\frac{\sqrt{2}}{2}$	0	0	0	0	0	0
$u_{B_{10}}^B$	0	$-\frac{\sqrt{2}}{2}$	$-\frac{\sqrt{2}}{2}$	0	0	0	0	0	0
$u_{B_{10}}^{1A}$	-1	0	0	0	0	0	0	0	0
$u_{B_{10}}^{2A}$	0	0	0	0	0	0	0	$\frac{\sqrt{2}}{2}i$	$-\frac{\sqrt{2}}{2}i$
$u_{B_{10}}^{1B}$	0	0	0	0	0	0	0	$\frac{\sqrt{2}}{2}i$	$\frac{\sqrt{2}}{2}i$
$u_{B_{10}}^{3A}$	0	0	0	0	0	0	$1i$	0	0
$u_{B_{10}}^{4A}$	0	0	0	0	$\frac{\sqrt{2}}{2}i$	$-\frac{\sqrt{2}}{2}i$	0	0	0
$u_{B_{10}}^{2B}$	0	0	0	0	$\frac{\sqrt{2}}{2}i$	$\frac{\sqrt{2}}{2}i$	0	0	0
$u_{B_{10}}^{5A}$	0	0	0	$1i$	0	0	0	0	0
$u_{B_{11}}^A$	0	$-\frac{\sqrt{2}}{2}$	$\frac{\sqrt{2}}{2}$	0	0	0	0	0	0

$u_{B_{11}}^B$	0	$-\frac{\sqrt{2}}{2}$	$-\frac{\sqrt{2}}{2}$	0	0	0	0	0	0
$u_{B_{11}}^{1A}$	1	0	0	0	0	0	0	0	0
$u_{B_{11}}^{2A}$	0	0	0	0	$-\frac{\sqrt{2}}{2}$	$\frac{\sqrt{2}}{2}$	0	0	0
$u_{B_{11}}^{1B}$	0	0	0	0	$-\frac{\sqrt{2}}{2}$	$-\frac{\sqrt{2}}{2}$	0	0	0
$u_{B_{11}}^{3A}$	0	0	0	1	0	0	0	0	0
$u_{B_{11}}^{4A}$	0	0	0	0	0	0	0	$-\frac{\sqrt{2}}{2}$	$\frac{\sqrt{2}}{2}$
$u_{B_{11}}^{2B}$	0	0	0	0	0	0	0	$-\frac{\sqrt{2}}{2}$	$-\frac{\sqrt{2}}{2}$
$u_{B_{11}}^{5A}$	0	0	0	0	0	0	1	0	0
$u_{\bar{B}_{11}}^A$	0	$\frac{\sqrt{2}}{2}$	$-\frac{\sqrt{2}}{2}$	0	0	0	0	0	0
$u_{\bar{B}_{11}}^B$	0	$\frac{\sqrt{2}}{2}$	$\frac{\sqrt{2}}{2}$	0	0	0	0	0	0
$u_{\bar{B}_{11}}^{1A}$	-1	0	0	0	0	0	0	0	0
$u_{\bar{B}_{11}}^{2A}$	0	0	0	0	0	0	0	$-\frac{\sqrt{2}}{2}i$	$\frac{\sqrt{2}}{2}i$
$u_{\bar{B}_{11}}^{1B}$	0	0	0	0	0	0	0	$-\frac{\sqrt{2}}{2}i$	$-\frac{\sqrt{2}}{2}i$
$u_{\bar{B}_{11}}^{3A}$	0	0	0	0	0	0	1i	0	0
$u_{\bar{B}_{11}}^{4A}$	0	0	0	0	$-\frac{\sqrt{2}}{2}i$	$\frac{\sqrt{2}}{2}i$	0	0	0
$u_{\bar{B}_{11}}^{2B}$	0	0	0	0	$-\frac{\sqrt{2}}{2}i$	$-\frac{\sqrt{2}}{2}i$	0	0	0
$u_{\bar{B}_{11}}^{5A}$	0	0	0	1i	0	0	0	0	0

- [1] K. Momma and F. Izumi, Journal of Applied Crystallography **44**, 1272 (2011).
- [2] H. Muta, Y. Murakami, M. Uno, K. Kurosaki, and S. Yamanaka, Journal of Nuclear Science and Technology **50**, 181 (2013).
- [3] K. Bakker, E. H. P. Cordfunke, R. J. M. Konings, and R. P. C. Schram, Journal of Nuclear Materials **250**, 1 (1997).
- [4] J. K. Fink, Journal of Nuclear Materials **279**, 1 (2000).
- [5] J. L. Bates, Nuclear Science and Engineering **21**, 26 (1965).
- [6] T. G. Godfrey, W. Fulkerson, T. G. Kollie, J. P. Moore, and D. L. McELROY, Journal of the American Ceramic Society **48**, 297 (1965).
- [7] C. Ronchi, M. Sheindlin, D. Staicu, and M. Kinoshita, Journal of Nuclear Materials **327**, 58 (2004).
- [8] P. M. Macedo, W. Capps, and J. O. Wachtman, Journal of the American Ceramic Society **47**, 651 (1964).
- [9] A. Khanolkar, Y. Wang, C. A. Dennett, Z. Hua, J. M. Mann, M. Khafizov, and D. H. Hurley, Journal of Applied Physics **133**, 195101 (2023).
- [10] O. G. Brandt and C. T. Walker, Physical Review Letters **18**, 11 (1967).